

SCIENTIFIC REPORTS

OPEN

New fluoroethyl phenylalanine analogues as potential LAT1-targeting PET tracers for glioblastoma

Jeroen Verhoeven¹, Fabian Hulpia², Ken Kersemans³, Julie Bolcaen³, Stef De Lombaerde¹, Jan Goeman⁴, Benedicte Descamps⁵, Giorgio Hallaert⁶, Caroline Van den Broecke⁷, Karel Deblaere⁸, Christian Vanhove⁵, Johan Van der Eycken⁴, Serge Van Calenbergh⁶, Ingeborg Goethals³ & Filip De Vos¹

The use of *O*-(2-[¹⁸F]fluoroethyl)-L-tyrosine ([¹⁸F]FET) as a positron emission tomography (PET) tracer for brain tumor imaging might have some limitations because of the relatively low affinity for the L-type amino acid transporter 1 (LAT1). To assess the stereospecificity and evaluate the influence of aromatic ring modification of phenylalanine LAT1 targeting tracers, six different fluoroalkylated phenylalanine analogues were synthesized. After *in vitro* K_i determination, the most promising compound, 2-[¹⁸F]-2-fluoroethyl-L-phenylalanine (2-[¹⁸F]FELP), was selected for further evaluation and *in vitro* comparison with [¹⁸F]FET. Subsequently, 2-[¹⁸F]FELP was assessed *in vivo* and compared with [¹⁸F]FET and [¹⁸F]FDG in a F98 glioblastoma rat model. 2-[¹⁸F]FELP showed improved *in vitro* characteristics over [¹⁸F]FET, especially when the affinity and specificity for system L is concerned. Based on our results, 2-[¹⁸F]FELP is a promising new PET tracer for brain tumor imaging.

In neuro-oncology, the potential of conventional magnetic resonance imaging (MRI) to differentiate neoplastic tissue from non-specific changes induced by treatment may be limited after therapeutic interventions (e.g. radiation therapy, neurosurgical resection, and chemotherapy). The molecular imaging modality positron emission tomography (PET) provides additional information on tumor metabolism, which allows for more accurate diagnostics and therapy response assessment^{1–3}. During the last decades, a variety of molecular targets have been assessed for brain tumor imaging by specific PET tracers. Especially amino acid (AA) based tracers received a lot of attention^{2,4}. In contrast to [¹⁸F]fluoro-2-deoxy-D-glucose ([¹⁸F]FDG, Fig. 1), the uptake of radiolabeled AAs is low in normal gray matter of the brain which results in higher tumor-to-background ratios⁵. A considerable advantage of AA over nucleoside- or choline-based tracers is the ability to pass through the intact blood-brain barrier (BBB) due to the presence of AA transporters. The transport of AA into cells is mediated by specific membrane associated carrier proteins, which are classified into different transporter systems based on criteria such as sodium dependence, substrate specificity, kinetics, etc.⁶. Amongst the currently known AA transporters, system L and system ASC are overexpressed in most tumor tissues, rendering these convenient targets for metabolic imaging of tumor cells^{7–9}. The most widespread ¹⁸F labeled tracers that have been developed are *O*-(2-[¹⁸F]fluoroethyl)-L-tyrosine ([¹⁸F]FET) and 3, 4-dihydroxy-6-[¹⁸F]-fluoro-L-phenylalanine ([¹⁸F]FDOPA; Fig. 1). Unfortunately, both are not specific for the L-type amino acid transporter 1 (LAT1) and the latter shows uptake in the striatum due to participation in the dopamine synthesis pathway^{10–13}. Most of the amino acid PET tracers, including [¹⁸F]FET, still suffer from various levels of physiological background uptake and uptake in non-neoplastic lesions such as acute inflammatory lesions as a result from multiple sclerosis or brain

¹Laboratory of Radiopharmacy, Ghent University, Ghent, Belgium. ²Laboratory for Medicinal Chemistry, Ghent University, Ghent, Belgium. ³Ghent University Hospital, Department of Nuclear Medicine, Ghent, Belgium. ⁴Laboratory for Organic and Bio-organic synthesis, Ghent University, Ghent, Belgium. ⁵IBiTech-MEDISIP Ghent University, Department of Electronics and Information Systems, Ghent, Belgium. ⁶Ghent University Hospital, Department of Neurosurgery, Ghent, Belgium. ⁷Ghent University Hospital, Department of Pathology, Ghent, Belgium. ⁸Ghent University Hospital, Department of Radiology and Medical Imaging, Ghent, Belgium. Correspondence and requests for materials should be addressed to J.V. (email: Jeroen.Verhoeven@ugent.be)

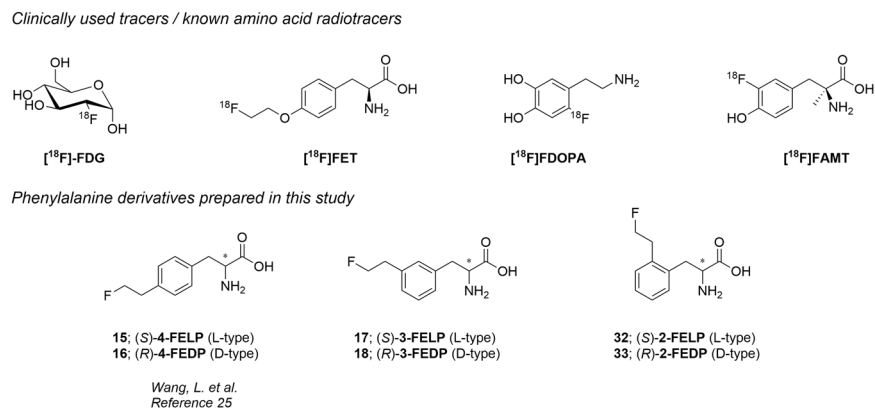


Figure 1. Structures of clinically used radiotracers or previously described amino acid tracers (upper part). Structures of the prepared modified phenylalanine analogs in this manuscript (lower part).

abscesses^{14–17}. An advantage of these non-natural amino acid tracers is the insusceptibility to *in vivo* metabolism resulting in the absence of radiolabeled metabolites¹⁸. Different PET and single-photon emission computed tomography (SPECT) tracers based on tyrosine, tryptophan and glutamine have been developed for LAT1 or ASCT2 targeting^{19–22}, of which the most promising results have been reported for 3-fluoro-L- α -methyltyrosine ($[^{18}\text{F}]$ FAMT, Fig. 1). However, the existing synthetic methods for the preparation of $[^{18}\text{F}]$ FAMT suffer from low chemical yields, which limits the availability of this tracer for clinical use^{23,24}. Based on the structure of $[^{18}\text{F}]$ FET, Wang *et al.* have developed *para*-fluoroethyl (15 & 16, Fig. 1) and -fluoropropyl alkylated phenylalanine derivatives, where the former showed appreciable uptake in the 9L glioma tumor model²⁵.

In this study we want to develop a practical synthesis for different phenylalanine derivatives and compare their affinity for the LAT1 transporter. As there are conflicting reports on the preferred stereochemistry of the phenylalanine/tyrosine analogues for the LAT1 transporter^{26–28}, both enantiomers (*S*) and (*R*) of *ortho*- (32 & 33) and *meta*- (17 & 18) substituted 2-fluoroethyl phenylalanine derivatives (Fig. 1) were synthesized and their K_i was determined in LAT1 overexpressing F98 glioblastoma (GB) cells²⁹. Previously reported *para*-substituted derivatives (15 & 16) were included to allow comparison with the novel analogs in our *in vitro* system. The *in vitro* uptake of the most promising compound was compared to $[^{18}\text{F}]$ FET and its uptake in a rat F98 GB model was evaluated.

Results

Chemistry. Initially, we set out to employ a common starting material (1 & 2, Fig. 2) to gain access to all the different (*ortho*-, *meta*- and *para*-) substituted phenylalanine amino acids. This approach was inspired by recent work of the Baran group, which described arylation of activated glutamate esters with boronic acids under Ni-catalysis³⁰. This route could enable access to all different phenylalanine derivatives from a single amino acid precursor.

The synthesis started from suitably protected commercially available L- or D-aspartic acid derivatives (Fig. 2). After activation of the side chain carboxylic acid as a N-hydroxytetrachlorophthalimide ester, 1 or 2 was reacted with the corresponding boronic acids (21 (*para*) or 22 (*meta*)) to give the substituted phenylalanine derivatives 3–6 in acceptable yields. The preparation of boronic acid derivatives is depicted in Fig. 3. Commercially available bromo-phenylethanol was protected with TBSCl and subsequently transformed into the corresponding boronic acid by Li/Br exchange and trapping with trimethylborate^{31,32}.

With the boronic acids in hand, cross-coupling was found successful for the synthesis of both *para*- and *meta*-substituted derivatives (Fig. 2). Next, the primary alcohol was unmasked by TBAF in THF, and fluorinated with DAST and deprotected to give rise to the fluorinated amino acids 15–18.

Attempts were made to prepare the *ortho*-substituted derivatives (32 & 33, Fig. 4) with the same strategy, however, this was met with several issues. Firstly, the preparation of TBS-protected *ortho*-boronic acid was troublesome, as the major product observed was the corresponding oxaborole (data not shown). This could be circumvented by employing the corresponding TIPS-protected alcohol. Next, the cross-coupling reaction with the *ortho*-substituted boronic acid failed to give appreciable amount of the coupled product, probably due to steric hindrance. This was confirmed by attempting the same reaction with commercially available 2-ethylphenylboronic acid and activated amino acid ester 1 under the same reaction conditions without success. Then, attempts with altered reaction conditions (temperature, catalyst loading and/or catalytic system (bathophenanthroline³⁰ instead of 4,4'-di-*tert*-butyl-2,2'-dipyridyl, BBBPY)) also did not deliver the desired product (data not shown). Therefore, it was decided to switch to another synthetic route, employing a pre-functionalized phenylalanine starting material (Fig. 4).

This synthetic approach was based on the literature route described for the synthesis of *para*-substituted phenylalanine amino acids^{25,28}. Commercially available N-Boc-2-bromophenylalanine was protected as its *tert*-butyl ester with *t*-butyl 2,2,2-trichloroacetimidate (TBTA) and vinyllated with a Stille coupling reaction to give 25 and 26. Next, hydroboration introduced the primary alcohol, which was either fluorinated and deprotected to give

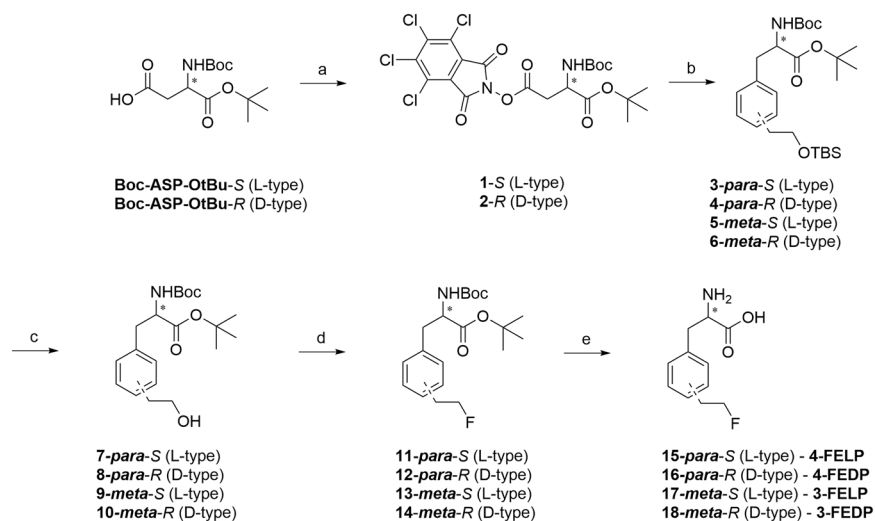


Figure 2. Reagents and conditions: a) TCNHPI, DIC, DCM, rt, 59% (**1**), 70% (**2**); b) Boronic acid (**21** or **22**), NiCl₂·6H₂O, BBP, Et₃N, DMF/1, 4-dioxane (1/10), 75 °C, overnight, 46% (**3** & **4**), 59% (**5**), 34% (**6**); c) 1 M TBAF in THF/THF, rt, 83% (**7**), 77% (**8**), 71% (**9**), 73% (**10**); d) DAST, DCM, 0 °C–rt, 42% (**11**), 37% (**12**), 50% (**13**), 29% (**14**); e) TFA/DCM (1/1), rt, 39% (**4-FELP**, **15**), 35% (**4-FEDP**, **16**), 46% (**3-FELP**, **17**), 46% (**3-FEDP**, **18**).

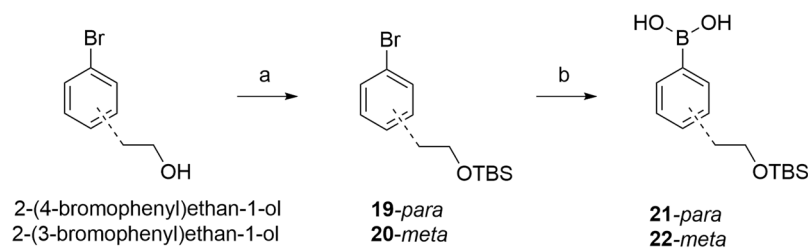


Figure 3. Reagents and conditions: a) TBSCl, imidazole, DME, 98% (**19**), quant. (**20**); b) i. n-BuLi (1.6 M in hexanes), THF, −78 °C; ii. B(OMe)₃, −78 °C–rt; iii. aq. HCl, 42% (**21**), 55% (**22**).

the free amino acids 2-FELP (**32**) and 2-FEDP (**33**), or tosylated with tosylchloride to give **31** to serve as radiolabelling precursor.

In vitro experiments. *Flow cytometry.* The expression of LAT1 in the F98 cells was confirmed by flow cytometry (Supplementary Fig. 4).

Concentration dependency using [2, 3, 4, 5, 6-³H]-L-phenylalanine. The affinity constant K_i of all compounds for the system L transporters was determined to identify the optimal derivatization position on the phenyl ring, as well as the preferred stereochemistry for system L targeting. The K_i-values are shown in Table 1 and representative K_m and K_{m,app} charts are shown in Fig. 5 (see also Supplementary Information). Between all compounds a statistically significant difference was found ($p = 0.002$), except between 3FEDP–3FELP and 3FEDP–4FELP ($p = 0.065$ and 0.485 respectively).

Radiochemistry. [¹⁸F]FET and 2-[¹⁸F]FELP were prepared as described below. Enantiomerically pure (ee > 99%) 2-[¹⁸F]FELP was synthesized in 90 min with high radiochemical purity (>95% as measured by analytical HPLC and TLC), good yield (10–30% with respect to the starting activity at the end of F18 production, not corrected for decay), and high molar activity (243.7 ± 11.9 GBq/μmol). Chromatograms can be found in the Supplementary Information.

2-[¹⁸F]FELP exhibits a logP_{oct} value of −1.16 ± 0.011 which is in accordance with the logP_{oct} value of phenylalanine (logP_{oct} = −1.38)³³ while a logP_{oct} value of −1.48 ± 0.047 was observed for [¹⁸F]FET.

Concentration and time dependency using 2-[¹⁸F]FELP or [¹⁸F]FET. Since the lowest K_i-value was obtained for 2-FELP, the uptake characteristics of this tracer were investigated further and compared with the uptake characteristics of FET (Fig. 6). The maximum uptake of [¹⁸F]FET, used as a reference, and 2-[¹⁸F]FELP was studied in F98 cells. The latter compound seemed more sodium dependent than [¹⁸F]FET (44% vs 36% more uptake in presence of Na⁺). BCH, a system L and b^{0,+} inhibitor, blocked the 2-[¹⁸F]FELP or [¹⁸F]FET uptake by >99% and 97%, respectively. In the presence of the system A inhibitor, MeAiB, 2-[¹⁸F]FELP was inhibited less (51.5% less uptake)

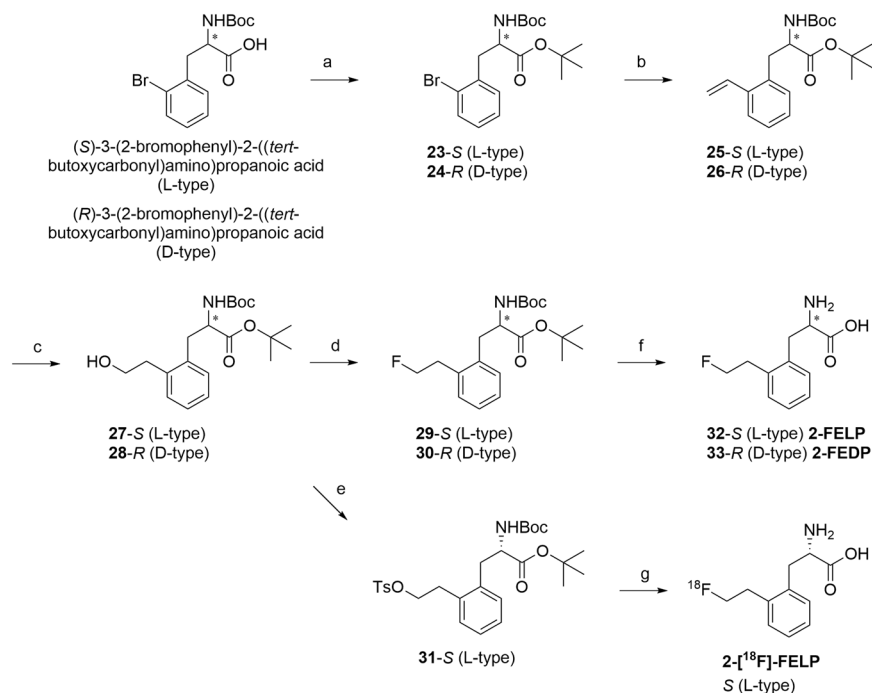


Figure 4. Reagents and conditions: a) TBTA, DCM, overnight, 90% (**23**), 72% (**24**); b) vinyl-Sn(nBu)₃, LiCl, Pd(Ph₃P)₂Cl₂, DMF, 70 °C, overnight, 51% (**25**), 67% (**26**); c) i. BH₃·THF, THF, 0 °C–rt; ii. NaBO₃·H₂O, water, rt, 66% (**27**), 61% (**28**); d) DAST, DCM, 0 °C–rt, 45% (**29**), 54% (**30**); e) Tosylchloride, DMAP, Et₃N, DCM, rt, 56% (**31**); f) TFA/DCM (1/1), rt, 23% (**2-FELP**, **32**), 49% (**2-FEDP**, **33**); g) i. [¹⁸F]F⁻/Kryptofix[®]222/K⁺ complex, MeCN, 100 °C, 15 min, ii. 2 M aq. HCl, 15 min, iii. 4 M aq. NaOH, iv. HPLC purification.

than that of [¹⁸F]FET (95% less uptake). The most interesting difference was observed by studying the effect of the recently developed LAT1 specific inhibitor JPH203, which inhibited the uptake of [¹⁸F]FET by 65% and that of 2-[¹⁸F]FELP by >99%. Statistical analysis showed a significant difference between the uptake in HEPES+ buffer and HEPES-/BCH/MeAiB/JPH203 ($p = 0.002$) and between BCH and MeAiB ($p = 0.002$) for both tracers. However, no difference could be found when the BCH and JPH203 uptake of 2-[¹⁸F]FELP ($p = 0.065$) was compared to [¹⁸F]FET ($p = 0.002$). These data indicate that LAT1 is more involved in the 2-[¹⁸F]FELP than in the [¹⁸F]FET uptake. The uptake in V_0 conditions of both 2-[¹⁸F]FELP and [¹⁸F]FET as a function of the concentration of non-radioactive analogue (0.01–0.5 mM) was saturable following the Michaelis-Menten equation. The related Michaelis-Menten plot resulted in a K_m value (expressed in μM , mean \pm SD, $n = 6$) of $12.54 \pm 3.82 \mu\text{M}$ for 2-[¹⁸F]FELP and $312.9 \pm 25.6 \mu\text{M}$ for [¹⁸F]FET. Moreover, the K_m values were not significantly different from their corresponding K_i values determined earlier (2-[¹⁸F]FELP: $p = 0.165$; [¹⁸F]FET: $p = 0.558$).

In vivo experiments. Two weeks after inoculation of F98 cells, tumors were visible in the right frontal region of rats on T2-weighted and contrast-enhanced T1-weighted MRI (Fig. 7). Hematoxylin and eosin stained paraffin sections revealed tumor necrosis, microvascular proliferation, nuclear atypia and increased mitosis, confirming the presence of GB (Fig. 8)^{11,34}.

Semi-quantitative analysis. The SUV_{mean} , SUV_{max} , TBR_{mean} and TBR_{max} were calculated for the different radiotracers (Fig. 9). No significantly different TBR and SUV values were found between 2-[¹⁸F]FELP and [¹⁸F]FET PET (TBR_{mean} : $p = 0.386$; TBR_{max} : $p = 0.773$; SUV_{mean} : $p = 0.0830$; SUV_{max} : $p = 1.00$). Significant differences were observed between 2-[¹⁸F]FELP and [¹⁸F]-FDG_{early} (TBR_{mean} : $p = 0.043$; TBR_{max} : $p = 0.021$; SUV_{mean} : $p = 0.021$), [¹⁸F]FET and [¹⁸F]FDG_{early} (TBR_{mean} : $p = 0.021$; TBR_{max} : $p = 0.021$), [¹⁸F]FET and [¹⁸F]FDG_{late} (TBR_{mean} : $p = 0.021$; SUV_{mean} : $p = 0.043$), [¹⁸F]FDG_{early} and [¹⁸F]FDG_{late} (TBR_{max} : $p = 0.043$; SUV_{mean} : $p = 0.043$). The TBR_{mean} values of the dynamic scans are shown in Fig. 10. The TBR_{mean} values of [¹⁸F]FDG PET scans were significantly lower in comparison with the 2-[¹⁸F]FELP and [¹⁸F]FET ($p = 0.043$ and 0.021 respectively). No significant differences were found between the AA PET scans ($p = 0.386$).

Discussion

The L-type AA transporter 1 transports aromatic or branched AA that are essential for cellular proliferation and growth. Due to its low expression and distribution in non-pathological cells and upregulation in glioma cells, this AA transporter received a lot of attention as potential target for tumor imaging^{1,13}. Molecular imaging using PET may provide relevant additional information on tumor metabolism and may be useful in case of ambiguous MRI findings following neuro-oncological treatment³⁵. In this study, two recently developed fluoroalkyl phenylalanine analogues, 4-FELP and 4-FEDP²⁵, together with four new compounds, 2-FELP, 2-FEDP, 3-FELP, 3-FEDP were

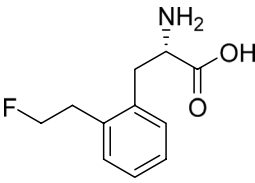
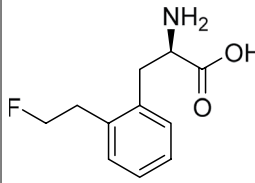
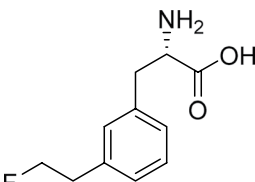
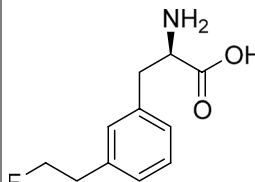
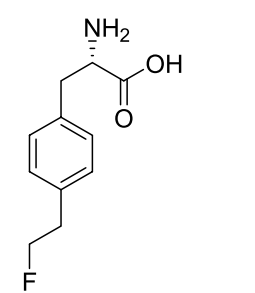
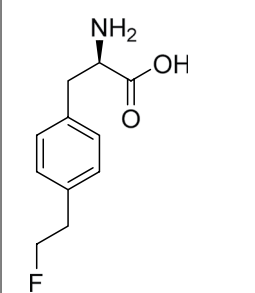
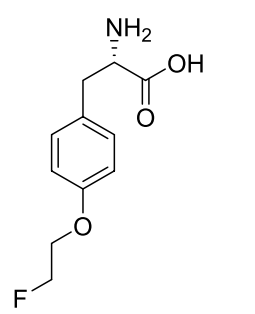
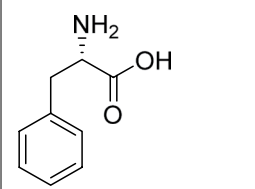
Compound	K _i value (μM)	Compound	K _i value (μM)
2FELP (analog 32, L-enantiomer) 	16.09 ± 3.74	2FEDP (analog 33, D-enantiomer) 	359.40 ± 47.10
3FELP (analog 17, L-enantiomer) 	48.95 ± 4.92	3FEDP (analog 18, D-enantiomer) 	83.75 ± 28.10
4FELP (analog 15, L-enantiomer) 	85.55 ± 4.40	4FEDP (analog 16, D-enantiomer) 	>2000
FET (L-enantiomer) 	307.20 ± 4.29	L-phenylalanine 	51.53 ± 7.80

Table 1. K_i values (expressed in μM, mean ± SD, n = 6) of the *ortho*-, *meta*- and *para*- substituted compounds, FET and L-phenylalanine.

successfully synthesized and compared *in vitro* to the reference compound FET, currently used in the clinic. The influence of the stereochemistry on the affinity for the LAT1 transporter was evaluated as there are some conflicting reports in literature. When comparing ^{123/125}I-labelled 2-iodo-L-phenylalanine and 2-iodo-D-phenylalanine in R1M cells²⁶, Kersemans *et al.* observed a high affinity of the LAT transporter for the D-enantiomer, while Bauwens *et al.*²⁷ reported a higher K_i values for D-tyrosine than for 2-I-L-tyrosine. In this study, the *in vitro* affinity of the D-enantiomers for the LAT1 transporter in F98 GB cells was lower than the affinity of the L-enantiomers, except for the *meta*-substituted enantiomers. This promiscuity regarding the (stereochemical) substrate preference was observed in a recent publication as well³⁶. When considering the K_i values of the L-enantiomers, the

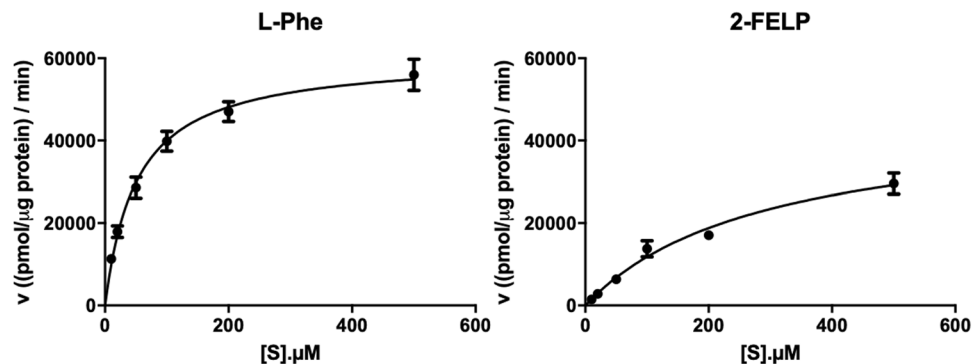


Figure 5. Left: Concentration dependence uptake of [^3H]-L-Phe. Right: Concentration dependence of [^3H]-L-Phe uptake in presence of 3-FELP. A 1-min incubation time was used. Michaelis-Menten plots were obtained to calculate K_m (left) and $K_{m,app}$ (right).

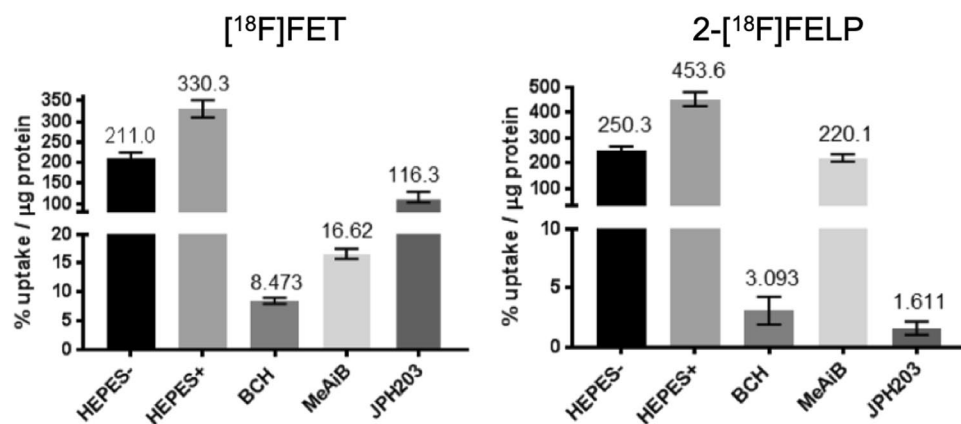


Figure 6. Maximum uptake of [^{18}F]FET and 2-[^{18}F]FELP in presence of sodium free (HEPES-) or sodium rich buffer (HEPES+) and supplemented with transporter specific inhibitors. Inhibitors: BCH for system L and $\text{b}^{0,+}$, MeAiB for system A, JPH203 for LAT1 (expressed as % uptake/ μg protein, mean \pm SD, $n = 6$).

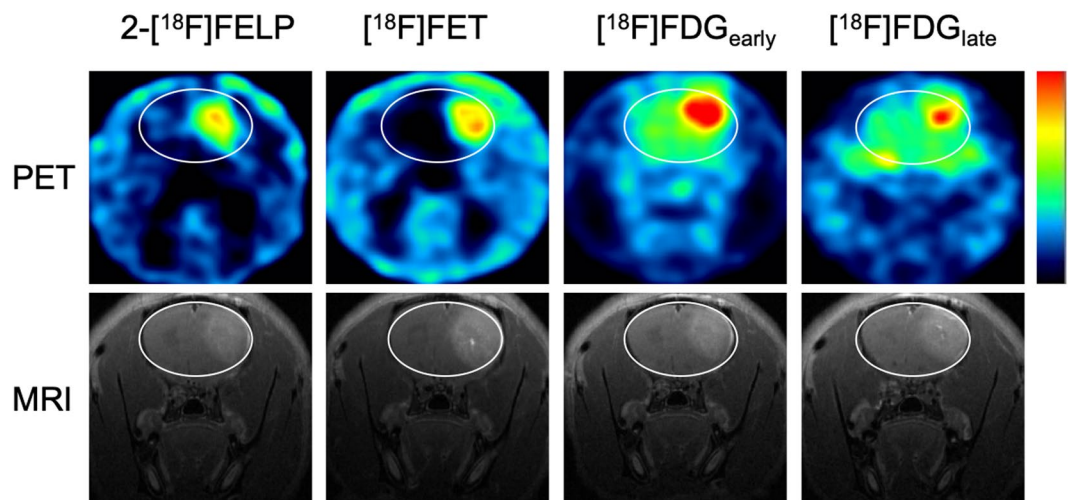


Figure 7. μPET images (upper row) and contrast-enhanced T1-weighted MRI (bottom row) of GB in rats. A high heterogeneous tumor uptake was visible on 2-[^{18}F]FELP (A) and [^{18}F]FET PET (B) (100–120 min post-injection) with a relative low uptake in healthy brain tissue. Both [^{18}F]FDG PET scans, 60 min (C) and 240 min post-injection (D), showed a homogeneous intense uptake in the tumor, however, a higher uptake in the surrounding normal brain tissue can be noted. The latter is clearly lower on the delayed [^{18}F]-FDG PET scan (D).

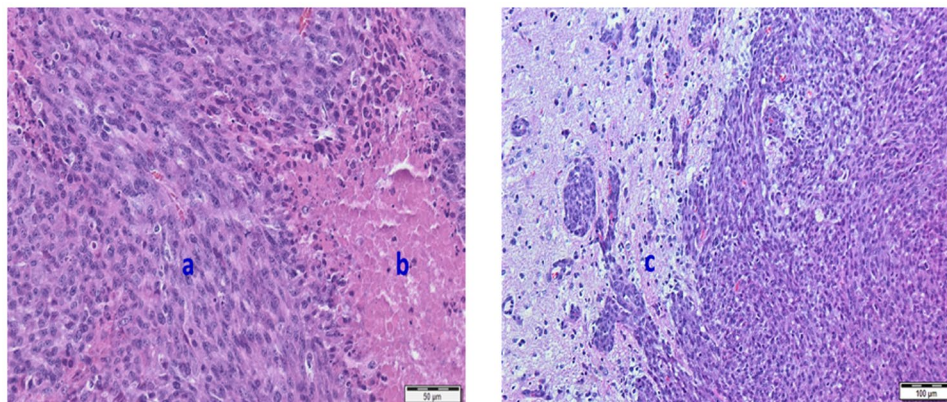


Figure 8. Hematoxylin and eosin stained paraffin sections of the rat brain confirming the presence of GB characteristics: High cellularity and nuclear pleiomorphism (a), microvascular proliferation and tumor necrosis (b), visible tumor infiltration with vessel recruitment at rim of tumor (c).

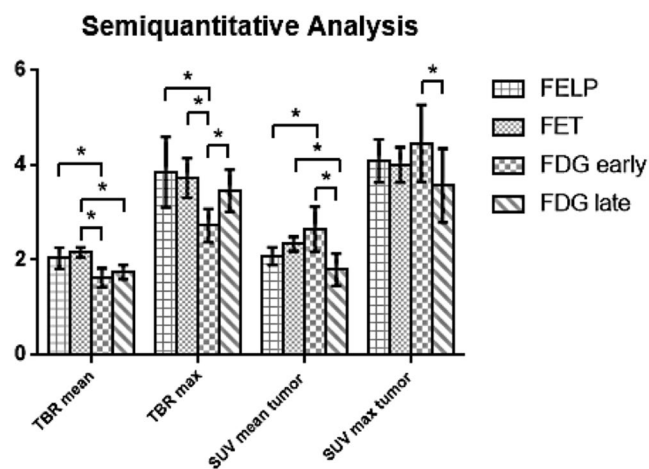


Figure 9. Comparison of the TBR_{mean}, TBR_{max}, SUV_{mean} and SUV_{max} in F98 GB tumor between 2-[¹⁸F]FELP, [¹⁸F]FET and [¹⁸F]FDG PET. **p* value < 0.05.

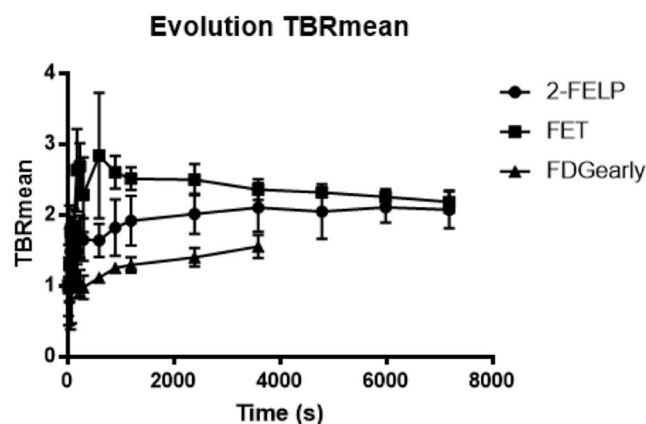


Figure 10. The TBR_{mean} values of the dynamic 2-[¹⁸F]FELP and [¹⁸F]FET PET scans were significantly higher in comparison with [¹⁸F]FDG. No significant differences were found between the AA PET scans.

preference of the position of the 2-fluoroethyl substituent on the aromatic ring of phenylalanine was as follows: *ortho* > *meta* > *para*.

Based on earlier studies^{36,37}, it has been shown that *meta*-substitution appears to be the most tolerant towards substitution. Therefore, it is quite remarkable that the *ortho*-substituted 2-FELP displays the highest *in vitro* affinity.

The radiofluorinated 2-^[18F]FELP and ^[18F]FET were successfully prepared on a Synthra RN plus module using identical reaction and purification conditions. The relatively straightforward synthesis method, as described earlier, simplifies the availability for clinical use, which has been an issue for ^[18F]FAMT³⁸.

In the present study, the *in vitro* influx of 2-^[18F]FELP and ^[18F]FET was characterized in F98 GB cells by means of inhibition experiments, involving the recently identified selective LAT1 inhibitor JPH203, which has structural analogy to tyrosine. Moreover, this compound effectively inhibits the proliferation of various tumor cells injected into nude mice³⁹. The uptake of 2-^[18F]FELP was considerably lower in presence of the inhibitor JPH203 compared to the uptake of ^[18F]FET. This indicates that 2-^[18F]FELP is predominantly transported by the LAT1 transporter. The results for ^[18F]FET are in conformity with the study conducted by Langen *et al.*⁴⁰ and the limited inhibition by JPH203 could be explained by LAT2 non-specific uptake, which has been described earlier in F98 cells⁴¹. As LAT1 overexpression has been correlated with malignant phenotype and proliferation of gliomas, our in-house developed AA could possibly demonstrate value for guiding biopsy, diagnosing primary brain tumor, tumor grading, directing radiotherapy, or even for discriminating between tumor recurrence and radionecrosis post-therapy^{42,43}.

In a second set of *in vitro* experiments, the K_m was determined by means of a concentration dependent assay. The results show a saturable transport consistent with Michaelis Menten kinetics. The K_i of 2-^[18F]FELP and ^[18F]FET did not differ significantly from their K_m values. The K_i value of a competitive inhibitor of a transport process of a substrate is equal to the K_m value for transport of the inhibitor by the same process. Therefore, the determination of K_i values can be particularly useful if no radioactive labeled compound is available⁴⁴.

Using an *in vivo* orthotopic tumor model, the uptake of different AA tracers were compared with ^[18F]FDG uptake characteristics. As described in literature, the AA tracers benefit from a lower background signal, resulting in increased tumor-to-background values³. However, no significant differences could be observed between 2-^[18F]FELP and ^[18F]FET. The elevated uptake of both tracers in the GB model could be enhanced by BBB breakdown⁴⁵. We hypothesize that the uptake in low grade glioma, where the BBB is intact and the LAT1 expression is less distinct, would give rise to different time activity curves as seen by Galdiks *et al.*⁴⁶. Unfortunately, preclinical low grade glioma models are not widely available⁴⁷.

In summary, 2-^[18F]FELP has a better affinity and selectivity for the LAT1 transporter compared to ^[18F]FET, decreasing non-specific tumor uptake. As LAT1 overexpression has been correlated with malignant phenotype and proliferation of gliomas, this new AA tracer could possibly demonstrate value for guiding biopsy, diagnosing primary brain tumor, tumor grading, directing radiotherapy, or even for discriminating between tumor recurrence and radionecrosis after initial therapy^{42,43}.

Conclusion

In this study we synthesized six fluoroalkyl substituted phenylalanine analogues, of which four have not been described before. The affinity of the D-enantiomers for the LAT1 transporter in F98 GB cells was lower than the affinity of the L-enantiomers. 2-FELP exhibits the best affinity for the F98 GB cells. Radiolabeling was performed on a Synthra RN plus module, following the same straightforward method as for ^[18F]FET. *In vitro* uptake and inhibition experiments showed that 2-^[18F]FELP is predominantly transported by the LAT1 transporter, decreasing non-specific uptake. No significantly different TBR_{mean} , TBR_{max} , SUV_{mean} tumor and SUV_{max} tumor values could be observed in comparison to ^[18F]FET in the F98 GB rat model. However, in contrast to ^[18F]FDG PET, higher TBRs were found. Based on our results, 2-^[18F]FELP is a promising new PET tracer for glioma or LAT1 imaging.

Methods

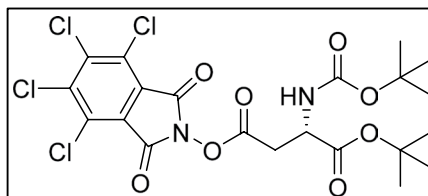
General. Reagents and solvents of analytical grade have been obtained from standard commercial sources and were used directly without further purification. Moisture sensitive reactions were performed under an argon atmosphere. Reactions were carried out at ambient temperature, unless specified in the text. For analytical TLC, pre-coated F254 aluminum plates (Machery-Nagel®) were employed, which have been visualized by UV and developed with sulfuric acid-anisaldehyde spray/charring. For purification, flash column chromatography was performed using Davisil® (40–63 μm) silica or a Reveleris X2 (Grace/Büchi) automated Flash unit with pre-packed cartridges. Exact mass was analyzed by means of a Waters LCT Premier XE™ Time of Flight (ToF) mass spectrometer with a standard electrospray (ESI) and modular Lockspray™ interface. Samples dissolved in an appropriate solvent system and infused in a MeCN/water (1:1) +0.1% formic acid mixture at 100 μL/min. NMR spectra were recorded on a Varian Mercury 300 MHz spectrometer. Chemical shifts (δ) are given in ppm and spectra are referenced to the residual solvent peak signal, with coupling constants (*J*) expressed in Hz. For ^{19F}-NMR, signals were referenced to the lock resonance frequency according to IUPAC referencing with CFCl₃ set to 0 ppm. Optical rotations were measured employing a Perkin Elmer 241 Polarimeter.

Chiral HPLC was performed using the specified chiral column (*vide infra*) from Diacel, 250 × 4.6 mm, particle size 5 μm. Column temperature was 35 °C. Runs were performed isocratically with a mixture of EtOH(abs.)/*n*-hexane as specified below, with a run length of 30 min at a flow rate of 1 mL/min.

Alternatively, chiral HPLC was performed (compounds **32** & **33**, including 2-^[18F]FELP) employing an Astec® Chirobiotic-T column (5 μm, 125 × 4.6 mm), operated at ambient temperature, with a mobile phase consisting of EtOH/water (8/2) at a flow rate of 1 mL/min.

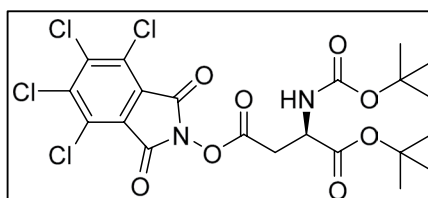
Chiral capillary electrophoresis (compounds **15** & **16** and **17** & **18**) was performed using a 64.5 cm capillary (50 μm diameter). The electrolyte used consisted of 25 mM phosphate buffer pH 2.5 + 5% HS-gammaCD chiral modifier. Analysis time was 40 min at -20 kV.

Experimental procedures & compound characterization data. 1-(*tert*-butyl)-4-(4, 5, 6, 7-tetrachloro-1, 3-dioxoisindolin-2-yl)-(tert-butoxycarbonyl)-L-aspartate (**1**).



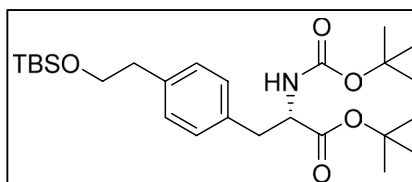
Boc-L-aspartic acid 4-*tert*-butyl ester (0.29 g, 1.0 mmol, 1 eq.) was dissolved in anhydrous DCM (10 mL, 10 mL/mmol SM). Then, DMAP (0.0012 g, 0.10 mmol, 0.1 eq.) and *N*-hydroxytetrachlorophthalimide (0.31 g, 1.0 mmol, 1 eq.) were added, followed by DIC (0.175 mL, 1.10 mmol, 1.1 eq.). The resulting suspension was stirred under argon for approximately 2 h. Then, the mixture was filtered and evaporated. Purification by column chromatography (0 \rightarrow 10% EA/PET) gave **1** (0.34 g, 0.59 mmol) as a white solid in 59% yield. $^1\text{H-NMR}$ (300 MHz, CDCl_3) δ : 1.46 (s, 9H, *t*Bu), 1.47 (s, 9H, *t*Bu), 3.23 (dd, $J = 17.4, 4.8$ Hz, 1H, CH_2), 3.32 (dd, $J = 17.4, 4.8$ Hz, 1H, CH_2), 4.57 (dt, $J = 7.2, 4.8$ Hz, 1H, CH), 5.47 (d, $J = 7.5$ Hz, 1H, NH). $^{13}\text{C NMR}$ (75 MHz, CDCl_3) δ : 27.9 (*t*-Bu, CH_3), 28.4 (*t*Bu, CH_3), 34.3 (CH_2), 50.3 (CHNH), 80.5 (*t*Bu-C-(CH_3) $_3$), 83.6 (*t*Bu-C-(CH_3) $_3$), 124.8, 130.7, 141.3, 155.5, 157.3, 167.2, 168.7. HRMS (ESI): calculated for $\text{C}_{21}\text{H}_{23}\text{Cl}_4\text{N}_1\text{O}_8$ ($[\text{M} + \text{H}]^+$): 571.0203, found: 571.0184. $[\alpha]^{20}_{\text{D}} = +37.76$ (c 1.17, CHCl_3).

Synthesis of 1-(*tert*-butyl) 4-(4, 5, 6, 7-tetrachloro-1, 3-dioxoisindolin-2-yl) (tert-butoxycarbonyl)-D-aspartate (**2**).



According to the procedure described for compound **1**; **Boc-D-aspartic acid 4-*tert*-butyl ester** (0.87 g, 3.0 mmol) was transformed into **2** (1.2 g, 2.1 mmol) as a white solid in 70% yield. $^1\text{H-NMR}$ (300 MHz, CDCl_3) δ : 1.46 (s, 9H, *t*Bu), 1.47 (s, 9H, *t*Bu), 3.23 (dd, $J = 17.4, 4.8$ Hz, 1H, CH_2), 3.32 (dd, $J = 17.4, 4.8$ Hz, 1H, CH_2), 4.56 (dt, $J = 7.2, 4.8$ Hz, 1H, CH), 5.46 (d, $J = 7.5$ Hz, 1H, NH). $^{13}\text{C NMR}$ (75 MHz, CDCl_3) δ : 27.9 (*t*Bu, CH_3), 28.4 (*t*Bu, CH_3), 34.3 (CH_2), 50.3 (CHNH), 80.5 (*t*Bu-C-(CH_3) $_3$), 83.6 (*t*Bu-C-(CH_3) $_3$), 124.8, 130.7, 141.3, 155.4, 157.3, 167.2, 168.7. HRMS (ESI): calculated for $\text{C}_{21}\text{H}_{23}\text{Cl}_4\text{N}_1\text{O}_8$ ($[\text{M} + \text{H}]^+$): 571.0203, found: 571.0234. $[\alpha]^{20}_{\text{D}} = -39.07$ (c 1.29, CHCl_3).

tert-butyl-(*S*)-2-((*tert*-butoxycarbonyl)amino)-3-(4-(2-((*tert*-butyldimethylsilyl)oxy)ethyl)phenyl)propanoate (**3** - *L*-type).



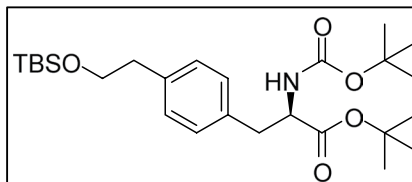
1 (0.477 g, 0.833 mmol, 1 eq.) and **21** (0.7 g, 2.5 mmol, 3 eq.) were placed in a 100 mL round bottom flask, equipped with a stir bar. The flask was evacuated and refilled with argon, three times. Then, anhydrous 1, 4-dioxane (33.8 mL, 40 mL/mmol SM) and Et_3N (1.16 mL, 8.33 mmol, 10 eq.) were added. The resulting mixture was stirred at ambient temperature until a homogeneous solution was obtained (~ 5 to 10 min). Then, the flask was transferred into a pre-heated oil bath at 75°C and stirred for another 5 min, after which the catalyst solution (3.4 mL, 4 mL/mmol SM) was added. The resulting solution was stirred at 75°C overnight. After cooling to ambient temperature, the solvents were removed *in vacuo*, and the residue taken up in EA/water. The layers were separated, and the water layer extracted twice with EA. The organic layers were combined, dried over Na_2SO_4 , filtered and evaporated. The residue was purified by column chromatography (0 \rightarrow 10% EA/PET) to give **3** (0.185 g, 0.386 mmol) as a yellowish oil in 46% yield. $^1\text{H-NMR}$ (300 MHz, CDCl_3) δ : -0.02 (s, 6H, Si- CH_3), 0.87 (s, 9H, Si-*t*Bu- CH_3), 1.42 (s, 18H, *t*Bu), 2.78 (t, $J = 7.2$ Hz, 2H, $\text{PhCH}_2\text{CH}_2\text{OTBS}$), 3.02 (d, $J = 5.7$ Hz, 2H, PhCH_2CHNH), 3.77 (t, $J = 7.2$ Hz, 2H, $\text{PhCH}_2\text{CH}_2\text{OTBS}$), 4.39–4.45 (m, 1H, CHNH), 4.94 (d, $J = 7.8$ Hz,

¹H, NH), 7.06–7.13 (m, 4H, H_{Phc}). ¹³C-NMR (75 MHz, CDCl₃) δ: –5.2 (2C, Si-CH₃), 18.5 (Si-C-(CH₃)₃), 26.1 (3C, Si-C-(CH₃)₃), 28.1 (3C, *t*Bu), 28.5 (3C, *t*Bu), 38.1 (Ph-CH₂CH), 39.4 (PhCH₂CH₂OTBS), 55.0 (CHNH), 64.7 (PhCH₂CH₂OTBS), 79.7 (*t*Bu-C-(CH₃)₃), 82.1 (*t*Bu-C-(CH₃)₃), 129.4 (2C), 129.5 (2C), 134.2, 137.9, 155.2 (C=O_{Boc}), 171.1 (C=O_{ester}). HRMS (ESI): calculated for C₂₆H₄₆NO₅Si ([M + H]⁺): 480.3140, found: 480.3138. [α]_D²⁰ = +26.78 (c 0.30, CHCl₃).

Chiral HPLC: Chiralpak IA, eluent: *n*-Hexane/EtOH(abs.) (97/3), retention time: 5.36 min. *ee*: 100%.

Preparation of the catalyst solution (NiCl₂·6H₂O; 4, 4-di-*t*-butyl-bipyridine 0.05 M in DMF) was performed as has been described in literature³⁰.

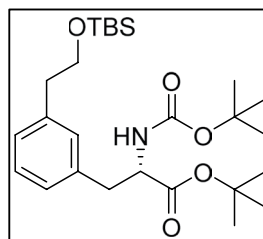
tert-butyl-(*R*)-2-((*tert*-butoxycarbonyl)amino)-3-(4-(2-((*tert*-butyldimethylsilyl)oxy)ethyl)phenyl)propanoate (4 - *D*-type).



According to the procedure described for 3; **2** (0.41 g, 0.71 mmol) was transformed into **4** (0.31 g, 0.65 mmol) as a colorless oil in 46% yield. ¹H-NMR (300 MHz, CDCl₃) δ: –0.02 (s, 6H, Si-CH₃), 0.87 (s, 9H, Si-*t*Bu-CH₃), 1.41 (s, 9H, *t*Bu), 1.42 (s, 9H, *t*Bu), 2.78 (t, *J* = 7.2 Hz, 2H, PhCH₂CH₂OTBS), 3.02 (d, *J* = 5.7 Hz, 2H, PhCH₂CH), 3.77 (t, *J* = 7.2 Hz, 2H, PhCH₂CH₂OTBS), 4.42 (dd, *J* = 13.8, 6.3 Hz, 1H, CHNH), 4.94 (d, *J* = 8.1 Hz, 1H, NHBoc), 7.05–7.13 (m, 4H, H_{Phc}). ¹³C-NMR (75 MHz, CDCl₃) δ: –5.3 (2C, Si-CH₃), 18.5 (Si-C-(CH₃)₃), 26.1 (3C, Si-C-(CH₃)₃), 28.1 (3C, *t*Bu), 28.5 (3C, *t*Bu), 38.1 (Ph-CH₂CH), 39.4 (PhCH₂CH₂OTBS), 55.0 (CHNH), 64.7 (PhCH₂CH₂OTBS), 79.7 (*t*Bu-C-(CH₃)₃), 82.1 (*t*Bu-C-(CH₃)₃), 129.3 (2C), 129.5 (2C), 134.2, 137.8, 155.2 (C=O_{Boc}), 171.1 (C=O_{ester}). HRMS (ESI): calculated for C₂₆H₄₆N₁O₅Si ([M + H]⁺): 480.3140, found: 480.3152. [α]_D²⁰ = –25.00 (c 0.56, CHCl₃).

Chiral HPLC: Chiralpak IA, eluent: *n*-Hexane/EtOH(abs.) (97/3), retention time: 4.95 min. *ee*: 96.3%.

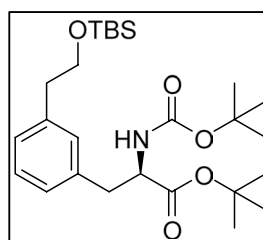
tert-butyl-(*S*)-2-((*tert*-butoxycarbonyl)amino)-3-(3-(2-hydroxyethyl)phenyl)propanoate (5 - *L*-type).



According to the procedure as described for 3; **1** (0.57 g, 1.0 mmol) was transformed into **5** (0.28 g, 0.59 mmol) as a colorless oil in 59% yield.

¹H-NMR (300 MHz, CDCl₃) δ: –0.01 (s, 6H, Si-(CH₃)₂), 0.87 (s, 9H, Si-*t*Bu-CH₃), 1.40 (s, 9H, *t*Bu), 1.42 (s, 9H, *t*Bu), 2.78 (t, *J* = 7.2 Hz, 2H, PhCH₂CH₂OTBS), 3.02 (d, *J* = 6.0 Hz, 2H, PhCH₂CH), 3.77 (t, *J* = 7.5 Hz, 2H, PhCH₂CH₂OTBS), 4.40–4.57 (m, 1H, CHNH_{Boc}), 4.96 (d, *J* = 7.8 Hz, 1H, NH_{Boc}), 6.99 (s, 1H, Ph-H), 7.02–7.09 (m, 2H, H_{Phc}), 7.19 (t, *J* = 7.5 Hz, 1H, H_{Phc}). ¹³C-NMR (75 MHz, CDCl₃) δ: –5.2 (2C, Si-CH₃), 18.5 (Si-C-(CH₃)₃), 26.1 (3C, Si-C-(CH₃)₃), 28.1 (*t*Bu, CH₃), 28.5 (*t*Bu, CH₃), 38.4 (PhCH₂CH), 39.7 (PhCH₂CH₂OTBS), 54.9 (CHNH), 64.7 (PhCH₂CH₂OTBS), 79.7 (*t*Bu-C-(CH₃)₃), 82.1 (*t*Bu-C-(CH₃)₃), 127.4, 127.8, 128.3, 130.5, 136.4, 139.2, 155.2 (C=O_{Boc}), 171.1 (C=O_{ester}). HRMS (ESI): calculated for C₂₆H₄₆NO₅Si ([M + H]⁺): 480.3140, found: 480.3142. [α]_D²⁰ = +26.76 (c 0.36, CHCl₃).

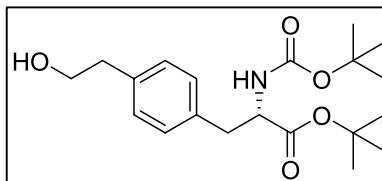
tert-butyl-(*R*)-2-((*tert*-butoxycarbonyl)amino)-3-(3-(2-hydroxyethyl)phenyl)propanoate (6 - *D*-type).



According to the procedure as described for 3; **2** (0.57 g, 1.0 mmol) was transformed into **6** (0.16 g, 0.34 mmol) as a colorless oil in 34% yield.

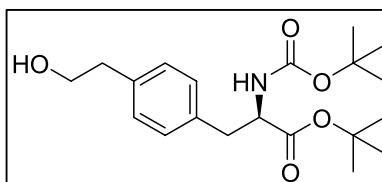
$^1\text{H-NMR}$ (300 MHz, CDCl_3) δ : -0.01 (s, 6H, $\text{Si}-(\text{CH}_3)_2$), 0.87 (s, 9H, $\text{Si}-t\text{Bu}-\text{CH}_3$), 1.40 (s, 9H, $t\text{Bu}$), 1.42 (s, 9H, $t\text{Bu}$), 2.78 (t, $J = 7.5$ Hz, 2H, $\text{PhCH}_2\text{CH}_2\text{OTBS}$), 3.03 (d, $J = 6.0$ Hz, 2H, PhCH_2CH), 3.78 (t, $J = 7.2$ Hz, 2H, $\text{PhCH}_2\text{CH}_2\text{OTBS}$), 4.40 – 4.47 (m, 1H, CHNH), 4.95 (d, $J = 7.8$ Hz, 1H, NH), 6.95 (s, 1H, H_{Phe}), 7.02 – 7.09 (m, 2H, H_{Phe}), 7.19 (t, $J = 7.8$ Hz, 1H, H_{Phe}). $^{13}\text{C-NMR}$ (75 MHz, CDCl_3) δ : -5.2 (2C, $\text{Si}-\text{CH}_3$), 18.5 ($\text{Si}-\text{C}-(\text{CH}_3)_3$), 26.1 (3C, $\text{Si}-\text{C}-(\text{CH}_3)_3$), 28.1 ($t\text{Bu}$), 28.5 (3C, $t\text{Bu}$), 38.5 (PhCH_2CH), 39.7 ($\text{PhCH}_2\text{CH}_2\text{OTBS}$), 54.9 (CHNH), 64.7 ($\text{PhCH}_2\text{CH}_2\text{OTBS}$), 79.7 ($t\text{Bu}-\text{C}-(\text{CH}_3)_3$), 82.1 ($t\text{Bu}-\text{C}-(\text{CH}_3)_3$), 127.5 , 127.8 , 128.3 , 130.5 , 136.4 , 139.2 , 155.2 ($\text{C}=\text{O}_{\text{Boc}}$), 171.1 ($\text{C}=\text{O}_{\text{ester}}$). HRMS (ESI): calculated for $\text{C}_{26}\text{H}_{46}\text{NO}_5\text{Si}$ ($[\text{M} + \text{H}]^+$): 480.3140 , found: 480.3183 . $[\alpha]_{\text{D}}^{20} = +24.07$ (c 0.26, CHCl_3).

tert-butyl-(S)-2-((tert-butoxycarbonyl)amino)-3-(4-(2-hydroxyethyl)phenyl)propanoate (7 - L-type).



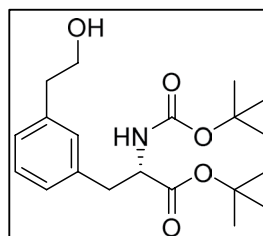
3 (0.098 g, 0.204 mmol) was dissolved in THF (3 mL, 10 mL/mmol SM) and TBAF in THF (1.0 M, 0.23 mL, 0.23 mmol, 1.1 eq.) was added. The resulting mixture was stirred for approximately 1H, and then sat. aq. NH_4Cl solution was added together with EA. The layers were separated; the water layer extracted twice more with EA. The organic layers were combined and dried over Na_2SO_4 , filtered and evaporated. The residue was purified by column chromatography (0 \rightarrow 35% EA/PET) to give **7** (0.062 g, 0.17 mmol) as a colorless oil in 83% yield. $^1\text{H-NMR}$ (300 MHz, CDCl_3) δ : 1.41 (s, 18H, $t\text{Bu}$), 1.62 (br. s, 1H, OH), 2.84 (t, $J = 6.6$ Hz, 2H, $\text{PhCH}_2\text{CH}_2\text{OH}$), 3.00 – 3.04 (m, 2H, PhCH_2CH), 3.84 (t, $J = 6.6$ Hz, 2H, $\text{PhCH}_2\text{CH}_2\text{OH}$), 4.43 (dd, $J = 14.1$, 6.6 Hz, 1H, PhCH_2CH), 4.98 (d, $J = 8.1$ Hz, 1H, NH), 7.10 – 7.26 (m, 4H, H_{Phe}). HRMS (ESI): calculated for $\text{C}_{20}\text{H}_{32}\text{NO}_5$ ($[\text{M} + \text{H}]^+$): 366.2275 , found: 366.2284 . $[\alpha]_{\text{D}}^{20} = +42.23$ (c 0.85, CHCl_3). Spectral data matched those reported in literature²⁵.

tert-butyl-(R)-2-((tert-butoxycarbonyl)amino)-3-(4-(2-hydroxyethyl)phenyl)propanoate (8 - D-type).



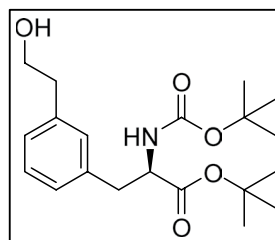
According to the procedure as described for **7**; **4** (0.326 g, 0.7 mmol) was transformed into **8** (0.196 g, 0.536 mmol) as a colorless oil in 77% yield. $^1\text{H-NMR}$ (300 MHz, CDCl_3) δ : 1.41 (s, 18H, $t\text{Bu}$), 2.84 (t, $J = 6.6$ Hz, 2H, $\text{PhCH}_2\text{CH}_2\text{OH}$), 2.96 – 3.08 (m, 2H, PhCH_2CH), 3.84 (t, $J = 6.6$ Hz, 2H, $\text{PhCH}_2\text{CH}_2\text{OH}$), 4.39 – 4.46 (m, 1H, CHNH), 4.98 (d, $J = 8.1$ Hz, 1H, NH), 7.10 – 7.17 (m, 4H, H_{Phe}). HRMS (ESI): calculated for $\text{C}_{20}\text{H}_{32}\text{NO}_5$ ($[\text{M} + \text{H}]^+$): 366.2275 , found: 366.2282 . Spectral data matched those reported in literature²⁵.

tert-butyl (S)-2-((tert-butoxycarbonyl)amino)-3-(3-(2-hydroxyethyl)phenyl)propanoate (9 - L-type).



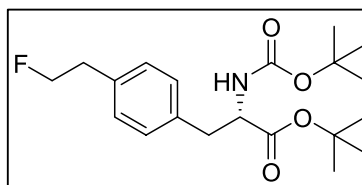
According to the procedure as described for **7**; **5** (0.547 g, 1.14 mmol) was transformed into **9** (0.29 g, 0.80 mmol) as a colorless oil in 71% yield. $^1\text{H-NMR}$ (300 MHz, CDCl_3) δ : 1.37 (s, 9H, $t\text{Bu}$), 1.42 (s, 9H, $t\text{Bu}$), 1.81 (br. s, 1H, OH), 2.82 (t, $J = 6.3$ Hz, 2H, $\text{PhCH}_2\text{CH}_2\text{OH}$), 2.92 (dd, $J = 13.8$, 6.9 Hz, 1H, PhCH_2CH), 3.10 (dd, $J = 13.8$, 6.0 Hz, 1H, PhCH_2CH), 3.76 – 3.90 (m, 2H, $\text{PhCH}_2\text{CH}_2\text{OH}$), 4.47 (dd, $J = 14.4$, 6.9 Hz, 1H, CHNH), 4.98 (d, $J = 8.7$ Hz, 1H, NH), 7.01 – 7.09 (m, 3H, H_{Phe}), 7.22 (t, $J = 7.8$ Hz, 1H, H_{Phe}). $^{13}\text{C-NMR}$ (75 MHz, CDCl_3) δ : 28.1 (3C, $t\text{Bu}$), 28.4 (3C, $t\text{Bu}$), 39.0 (PhCH_2CH), 39.3 ($\text{PhCH}_2\text{CH}_2\text{OH}$), 55.0 (PhCH_2CH), 63.7 ($\text{PhCH}_2\text{CH}_2\text{OH}$), 79.8 ($t\text{Bu}-\text{C}-(\text{CH}_3)_3$), 82.2 ($t\text{Bu}-\text{C}-(\text{CH}_3)_3$), 127.6 , 128.0 , 128.7 , 130.5 , 136.8 , 138.8 , 155.1 ($\text{C}=\text{O}_{\text{Boc}}$), 171.2 ($\text{C}=\text{O}_{\text{ester}}$). HRMS (ESI): calculated for $\text{C}_{20}\text{H}_{32}\text{NO}_5$ ($[\text{M} + \text{H}]^+$): 366.2275 , found: 366.2268 . $[\alpha]_{\text{D}}^{20} = +25.68$ (c 0.51, CHCl_3).

Chiral HPLC: Chiralpak IB, eluent: *n*-Hexane/EtOH(abs.) (97/3), retention time: 12.39 min. *ee*: 99.6%.

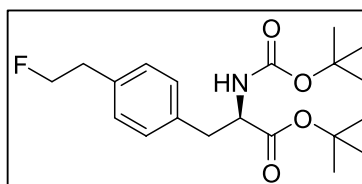
tert-butyl-(*R*)-2-((*tert*-butoxycarbonyl)amino)-3-(3-(2-hydroxyethyl)phenyl)propanoate (*10* - *D*-type).

According to the procedure as described for **7**; **6** (0.26 g, 0.54 mmol) was transformed into **10** (0.15 g, 0.40 mmol) as a colorless oil in 73% yield. ^1H -NMR (300 MHz, CDCl_3) δ : 1.37 (s, 9H, *t*Bu), 1.44 (s, 9H, *t*Bu), 1.94 (br. s, 1H, OH), 2.82 (t, $J = 6.6$ Hz, 2H, Ph- CH_2CH), 2.92 (dd, $J = 13.8, 6.9$ Hz, 1H, Ph CH_2CH), 3.09 (dd, $J = 13.8, 5.7$ Hz, 1H, Ph CH_2CH), 3.75–3.89 (m, 2H, Ph $\text{CH}_2\text{CH}_2\text{OH}$), 4.46 (dd, $J = 14.4, 6.9$ Hz, 1H, CHNH), 4.99 (d, $J = 8.1$ Hz, 1H, NH), 7.00–7.09 (m, 3H, H_{Ph}), 7.21 (t, $J = 7.8$ Hz, 1H, H_{Ph}). ^{13}C -NMR (75 MHz, CDCl_3) δ : 28.1 (3C, *t*Bu), 28.4 (3C, *t*Bu), 38.9 (Ph CH_2CH), 39.3 (Ph $\text{CH}_2\text{CH}_2\text{OH}$), 55.0 (Ph CH_2CH), 63.7 (Ph $\text{CH}_2\text{CH}_2\text{OH}$), 79.8 (*t*Bu-C-(CH_3)₃), 82.2 (*t*Bu-C-(CH_3)₃), 127.6, 127.9, 128.6, 130.5, 136.7, 138.8, 155.1 (C=O_{Boc}), 171.1 (C=O_{ester}). HRMS (ESI): calculated for $\text{C}_{20}\text{H}_{32}\text{N}_1\text{O}_5$ ($[\text{M} + \text{H}]^+$): 366.2275, found: 366.2281. $[\alpha]_{\text{D}}^{20} = -26.79$ (c 0.52, CHCl_3).

Chiral HPLC: Chiralpak IB, eluent: *n*-Hexane/EtOH(abs.) (97/3), retention time: 10.52 min. *ee*: 98.3%.

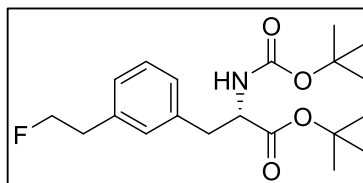
tert-butyl-(*S*)-2-((*tert*-butoxycarbonyl)amino)-3-(4-(2-fluoroethyl)phenyl)propanoate (*11* - *L*-type).

7 (0.18 g, 0.49 mmol, 1 eq.) was dissolved in anhydrous DCM (2.5 mL, 10 mL/mmol SM) under argon and cooled in an ice bath at 0 °C. Then, DAST (0.20 mL, 1.5 mmol, 3 eq.) was added dropwise and the resulting solution stirred at ambient temperature for 3–4 h. Then, the mixture was cooled to 0 °C in an ice bath and aq. sat. NaHCO_3 solution was added dropwise. After the gas evolution ceased, the mixture was transferred into a separatory funnel and more sat. aq. NaHCO_3 solution was added. The layers were separated, and the water layer was extracted twice more with DCM. The organic layers were combined, dried over Na_2SO_4 , filtered and evaporated till dryness. The resulting mixture was purified by column chromatography (0 → 12% EA/PET) to give **11** (0.076 g, 0.21 mmol) as a colorless oil in 42% yield. ^1H -NMR (300 MHz, CDCl_3) δ : 1.40 (s, 9H, *t*Bu), 1.42 (s, 9H, *t*Bu), 2.94 (t, $J = 6.6$ Hz, 1H, Ph $\text{CH}_2\text{CH}_2\text{F}$)*, 3.00–3.06 (m, 3H, Ph $\text{CH}_2\text{CH}_2\text{F}$; Ph CH_2CH), 4.43 (q, $J = 6.9$ Hz, 1H, Ph CH_2CH), 4.60 (dt, $J = 47.1, 6.6$ Hz, 2H, Ph $\text{CH}_2\text{CH}_2\text{F}$), 4.98 (d, $J = 6.9$ Hz, 1H, NH), 7.10–7.17 (m, 4H, H_{Ph}). ^{19}F -NMR (282 MHz, CDCl_3) δ : -214.98 – -215.48 (m, 1F). Spectral data are in accordance with literature values²⁵.

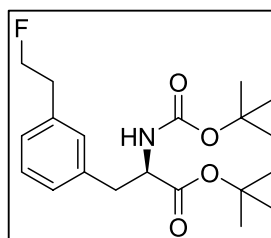
tert-butyl-(*R*)-2-((*tert*-butoxycarbonyl)amino)-3-(4-(2-fluoroethyl)phenyl)propanoate (*12* - *D*-type).

According to the procedure described for **11**; **8** (0.174 g, 0.476 mmol) was transformed into **12** (0.065 g, 0.18 mmol) as a colorless oil in 37% yield. ^1H -NMR (300 MHz, CDCl_3) δ : 1.40 (s, 9H, *t*Bu), 1.42 (s, 9H, *t*Bu), 2.98 (dt, $J = 23.1, 6.6$ Hz, 2H, Ph $\text{CH}_2\text{CH}_2\text{F}$), 3.00–3.04 (m, 2H, Ph CH_2CH), 4.43 (dd, $J = 13.8, 6.3$ Hz, 1H, Ph CH_2CH), 4.60 (dt, $J = 47.1, 6.9$ Hz, 2H, Ph $\text{CH}_2\text{CH}_2\text{F}$), 4.98 (d, $J = 8.4$ Hz, 1H, NH), 7.10–7.17 (m, 4H, H_{Ph}). ^{19}F -NMR (282 MHz, CDCl_3) δ : -214.98 – -215.48 (m, 1F). Spectral data matched those reported in literature²⁵.

*This peak is in fact a doublet of triplets (F-coupling); however, the peak coincides with the PhCH₂CH signal and was not sufficiently resolved for adequate calculation.

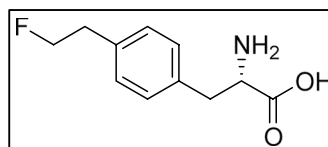
tert-butyl-(*S*)-2-((*tert*-butoxycarbonyl)amino)-3-(3-(2-(*tosyloxy*)ethyl)phenyl)propanoate (**13** - *L*-type).

According to the procedure described for **11**; **9** (0.235 g, 0.634 mmol) was transformed into **13** (0.117 g, 0.319 mmol) as a colorless oil in 50% yield. $^1\text{H-NMR}$ (300 MHz, CDCl_3) δ : 1.40 (s, 9H, *t*Bu), 1.42 (s, 9H, *t*Bu), 2.98 (dt, $J = 23.1, 6.6$ Hz, 2H, $\text{PhCH}_2\text{CH}_2\text{F}$), 3.03 (dd, $J = 6.3, 4.2$ Hz, 2H, PhCH_2CHNH), 4.41–4.48 (m, 1H, PhCH_2CH), 4.61 (dt, $J = 47.1, 6.6$ Hz, 2H, $\text{PhCH}_2\text{CH}_2\text{F}$), 4.98 (d, $J = 7.8$ Hz, 1H, NH), 7.04–7.12 (m, 3H, H_{phe}), 7.22 (d, $J = 7.8$ Hz, 1H, H_{phe}). $^{19}\text{F-NMR}$ (282 MHz, CDCl_3) δ : -215.06 (tt, $J = 46.8, 22.8$ Hz, 1F). $^{13}\text{C-NMR}$ (75 MHz, CDCl_3) δ : 28.1 (3C, *t*Bu), 28.5 (3C, *t*Bu), 37.0 (d, $J = 20.6$ Hz, 1C, $\text{PhCH}_2\text{CH}_2\text{F}$), 38.6 (PhCH_2CHNH Boc), 54.9 (PhCH_2CHNH), 79.8 (*t*Bu-C-(CH_3)₃), 82.2 (*t*-Bu-C-(CH_3)₃), 84.1 (d, $J = 168.2$ Hz, 1C, $\text{PhCH}_2\text{CH}_2\text{F}$), 127.6, 128.0, 128.7, 130.4, 136.8, 137.2 (d, $J = 5.7$ Hz, 1C, $\text{Ph-C-CH}_2\text{CH}_2\text{F}$), 155.2 (C=O_{Boc}), 171.1 (C=O_{ester}). HRMS (ESI): calculated for $\text{C}_{20}\text{H}_{31}\text{FNO}_4$ ($[\text{M} + \text{H}]^+$): 368.2232, found: 368.2231. $[\alpha]_{\text{D}}^{20} = +40.83$ (c 0.72, CHCl_3).

tert-butyl-(*R*)-2-((*tert*-butoxycarbonyl)amino)-3-(3-(2-hydroxyethyl)phenyl)propanoate (**14** - *D*-type).

According to the procedure described for **11**; **10** (0.146 g, 0.399 mmol) was transformed into **14** (0.042 g, 0.11 mmol) as a colorless oil in 29% yield.

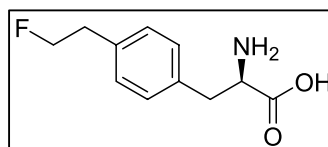
$^1\text{H-NMR}$ (300 MHz, CDCl_3) δ : 1.40 (s, 9H, *t*Bu), 1.42 (s, 9H, *t*Bu), 2.95 (dt, $J = 23.1, 6.6$ Hz, 2H, $\text{PhCH}_2\text{CH}_2\text{F}$), 3.01–3.05 (m, 2H, PhCH_2CHNH), 4.45 (dd, $J = 14.1, 6.3$ Hz, 1H, PhCH_2CHNH), 4.61 (dt, $J = 47.1, 6.6$ Hz, 2H, $\text{PhCH}_2\text{CH}_2\text{F}$), 4.99 (d, $J = 8.1$ Hz, 1H, NH), 7.04–7.12 (m, 3H, H_{phe}), 7.22 (d, $J = 7.2$ Hz, 1H, H_{phe}). $^{19}\text{F-NMR}$ (282 MHz, CDCl_3) δ : -215.02 (tt, $J = 46.8, 22.8$ Hz, 1F). $^{13}\text{C-NMR}$ (75 MHz, CDCl_3) δ : 28.1 (3C, *t*Bu), 28.5 (3C, *t*Bu), 37.0 (d, $J = 20.63$ Hz, 1C, $\text{PhCH}_2\text{CH}_2\text{F}$), 38.5 (PhCH_2CHNH), 54.9 (PhCH_2CHNH), 79.8 (*t*Bu-C-(CH_3)₃), 82.2 (*t*Bu-C-(CH_3)₃), 84.1 (d, $J = 168.3$ Hz, 1C, $\text{PhCH}_2\text{CH}_2\text{F}$), 127.6, 128.0, 128.7, 130.4, 136.8, 137.2 (d, $J = 5.7$ Hz, 1C, $\text{Ph-C-CH}_2\text{CH}_2\text{F}$), 155.2 (C=O_{Boc}), 171.1 (C=O_{ester}). HRMS (ESI): calculated for $\text{C}_{20}\text{H}_{31}\text{FN}_2\text{O}_4$ ($[\text{M} + \text{H}]^+$): 368.2232, found: 368.2228. $[\alpha]_{\text{D}}^{20} = -40.24$ (c 0.4, CHCl_3).

(S)-2-amino-3-(4-(2-fluoroethyl)phenyl)propanoic acid (**15** - *L*-type - 4FELP).

11 (0.076 g, 0.21 mmol) was dissolved in DCM (3.0 mL) after which TFA (3.0 mL) was added. The resulting solution was stirred at ambient temperature for approximately 5 hours, after which it was evaporated till dryness. Next, the residue was co-evaporated with MeOH three times. Then, the residue was dissolved in ~2 mL of MeOH and the pH was adjusted to pH 6–7, with diluted aq. NH_3 solution, after which a white precipitate formed. The mixture was refrigerated overnight, and then the liquid was removed via pipette aspiration. The remaining solid was washed thrice with a minimal amount of ice-cold MeOH and dried by means of oil pump high vacuum to give **15** (0.017 g, 0.081 mmol) as a white powder in 39% yield. $^1\text{H-NMR}$ (300 MHz, D_2O) δ : 3.06 (dt, $J = 27.6, 6.3$ Hz, 2H, $\text{PhCH}_2\text{CH}_2\text{F}$), 3.12 (dd, $J = 14.4, 8.1$ Hz, 1H, $\text{PhCH}_2\text{CHNH}_2$), 3.29 (dd, $J = 14.7, 5.4$ Hz, 1H, $\text{PhCH}_2\text{CHNH}_2$), 3.99 (dd, $J = 8.1, 5.4$ Hz, 1H, $\text{PhCH}_2\text{CHNH}_2$), 4.67 (t, $J = 6.0$ Hz, 1H, $\text{PhCH}_2\text{CH}_2\text{F}$), 7.29–7.37 (m, 4H, H_{phe}). $^{19}\text{F-NMR}$ (282 MHz, D_2O) δ : -214.75 (tt, $J = 49.8, 29.4$ Hz, 1F). HRMS (ESI): calculated for $\text{C}_{11}\text{H}_{15}\text{FNO}_2$ ($[\text{M} + \text{H}]^+$): 212.1081, found: 212.1077.

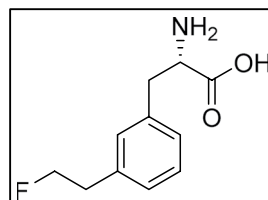
Chiral CE: retention time: 32.6 min, *ee*: 98.5%.

1 proton signal is missing ($\text{PhCH}_2\text{CH}_2\text{F}$) as it resides under the HDO peak; therefore, the signal for $\delta = 4.67$ ppm is calculated on the visual triplet and not on the actual doublet of triplets (dt).

(R)-2-amino-3-(4-(2-fluoroethyl)phenyl)propanoic acid (**16** - *D*-type - 4-FEDP).

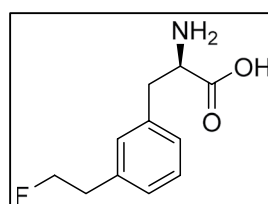
According to the procedure as described for **15**; **11** (0.065 g, 0.18 mmol) was transformed into **11** (0.013 g, 0.062 mmol) as a white powder in 35% yield. $^1\text{H-NMR}$ (300 MHz, D_2O) δ : 3.06 (dt, $J = 27.6, 6.0$ Hz, 2H, $\text{PhCH}_2\text{CH}_2\text{F}$), 3.12 (dd, $J = 14.7, 8.1$ Hz, 1H, PhCH_2CH), 3.29 (dd, $J = 14.7, 5.4$ Hz, 1H, $\text{PhCH}_2\text{CHNH}_2$), 3.99 (dd, $J = 8.1, 5.4$ Hz, 1H, $\text{PhCH}_2\text{CHNH}_2$), 4.75 (dt, $J = 47.1, 6.3$ Hz, 2H, $\text{PhCH}_2\text{CH}_2\text{F}$), 7.29–7.37 (m, 4H, H_{phe}). $^{19}\text{F-NMR}$ (282 MHz, D_2O) δ : -216.04 (tt, $J = 44.8, 29.1$ Hz, 1F).

Chiral CE: retention time: 28.4 min, *ee*: 88.8%.

(S)-2-amino-3-(3-(2-fluoroethyl)phenyl)propanoic acid.HCl salt (**17** - *L*-type - 3-FELP).

13 (0.114 g, 0.310 mmol) was dissolved in DCM (3.0 mL) after which TFA (3.0 mL) was added. The resulting solution was stirred at ambient temperature for approximately 5 hours. Then, the mixture was evaporated till dryness. The mixture was co-evaporated with MeOH three times. Then, the residue was neutralized with diluted aq. NH_3 and refrigerated. As no precipitate formed; the mixture was evaporated till dryness and dissolved in water (~5 mL); and the pH adjusted to pH 6. Then, the mixture was purified by RP-flash chromatography (4 g, C-18 column, Büchi). Gradient: 100% water for 1 min, then linear gradient 0 → 20% EtOH/water in 15 min. Product containing fractions were pooled and most of the water was evaporated *in vacuo*; after which the residue was lyophilized. Then, the white powder was dissolved in water and diluted (~0.5 M) aq. HCl (~0.5 mL) was added and lyophilized again, which gave **17** (0.035 g, 0.14 mmol) as a white powder in 46% yield. $^1\text{H-NMR}$ (300 MHz, D_2O) δ : 3.06 (dt, $J = 27.9, 6.0$ Hz, 2H, $\text{PhCH}_2\text{CH}_2\text{F}$), 3.21 (dd, $J = 14.4, 7.8$ Hz, 1H, PhCH_2CH), 3.35 (dd, $J = 14.4, 5.7$ Hz, 1H, PhCH_2CH), 4.28 (dd, $J = 7.8, 5.7$ Hz, 1H, PhCH_2CH), 4.75 (dt, $J = 46.8, 6.0$ Hz, 2H, $\text{PhCH}_2\text{CH}_2\text{F}$), 7.23–7.34 (m, 3H, H_{phe}), 7.41 (t, $J = 7.5$ Hz, 1H, H_{phe}). $^{19}\text{F-NMR}$ (282 MHz, D_2O) δ : -216.11 (tt, $J = 46.8, 27.6$ Hz, 1F). $^{13}\text{C-NMR}$ (75 MHz, D_2O) δ : 35.6 (PhCH_2CH), 35.8 (d, $J = 19.4$ Hz, 1C, $\text{PhCH}_2\text{CH}_2\text{F}$), 54.5 (PhCH_2CH), 85.1 (d, $J = 160.3$ Hz, 1C, $\text{PhCH}_2\text{CH}_2\text{F}$), 127.6, 128.4, 129.3, 129.9, 134.5, 138.7 (d, $J = 4.6$ Hz, 1C, $\text{Ph-CH}_2\text{CH}_2\text{F}$), 171.8 (C=O). HRMS (ESI): calculated for $\text{C}_{11}\text{H}_{15}\text{FNO}_2$ ($[\text{M} + \text{H}]^+$): 212.1081, found: 212.1046.

Chiral CE: retention time: 23.74 min, *ee*: 95.4%.

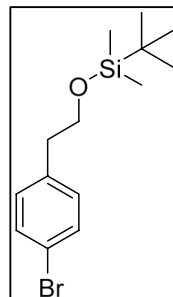
(R)-2-amino-3-(3-(2-fluoroethyl)phenyl)propanoic acid.HOAc salt (**18** - *D*-type - 3-FEDP).

14 (0.072 g, 0.20 mmol) was dissolved in DCM (2.0 mL) after which TFA (2.0 mL) was added. The resulting solution was stirred at ambient temperature for approximately 5 hours. Then, the mixture was evaporated till dryness. The mixture was co-evaporated with MeOH three times. Then, the residue was neutralized with diluted aq. NH_3 and refrigerated. As no precipitate formed; the mixture was evaporated till dryness and dissolved in water (~4 mL); and the pH adjusted to pH 6. Then, the mixture was purified by RP-flash chromatography (4 g, C-18 column, Büchi). Gradient: 100% water for 1 min, then linear gradient 0 → 20% EtOH/water in 15 min. Product containing fractions were pooled and most of the water was evaporated *in vacuo*; after which the residue was lyophilized. Then, the white powder was dissolved in water and diluted (~0.5 M) aq. HOAc (~0.5 mL) was added and lyophilized again, which gave **18** (0.025 g, 0.092 mmol) as a white powder in 46% yield. $^1\text{H-NMR}$ (300 MHz, D_2O) δ : 1.97 (s, 3H, OAc), 3.06 (dt, $J = 27.9, 6.3$ Hz, 2H, $\text{PhCH}_2\text{CH}_2\text{F}$), 3.12 (dd, $J = 15.0, 5.7$ Hz, 1H, PhCH_2CH), 3.29 (dd, $J = 14.7, 5.4$ Hz, 1H, PhCH_2CH), 4.00 (dd, $J = 8.1, 5.1$ Hz, 1H, PhCH_2CH), 4.75 (dt, $J = 47.1, 6.3$ Hz, 2H, $\text{PhCH}_2\text{CH}_2\text{F}$), 7.21–7.32 (m, 3H, H_{phe}), 7.40 (t, $J = 7.5$ Hz, 1H, H_{phe}). $^{19}\text{F-NMR}$ (282 MHz, D_2O) δ : -215.90 (tt, $J = 46.8, 27.6$ Hz, 1F). $^{13}\text{C-NMR}$ (75 MHz, D_2O) δ : 22.5 (CH_3 -acetate), 35.8 (d, $J = 19.5$ Hz, 1C, $\text{PhCH}_2\text{CH}_2\text{F}$), 36.2 (PhCH_2CH), 55.9 (PhCH_2CH), 85.1 (d, $J = 161.48$ Hz, 1C, $\text{PhCH}_2\text{CH}_2\text{F}$), 127.5, 128.2, 129.2, 129.8, 135.4, 138.6

(d, $J=4.6$ Hz, 1C, Ph-C-CH₂CH₂F), 173.8 (C=O), 180.2 (C=O, acetate). HRMS (ESI): calculated for C₁₁H₁₅FNO₂ ([M + H]⁺): 212.1081, found: 212.1079.

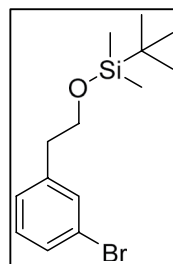
Chiral CE: retention time: 19.3 min, *ee*: 93.8%.

*Synthesis of 4-bromophenethoxy(*t*-butyl)dimethylsilane (19) 2-(4-bromophenyl)-ethanol.*



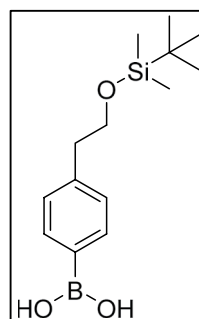
(2.0 g, 10 mmol, 1 eq.) was dissolved in 20 mL anhydrous DMF (2 mL/mmol SM) under argon. Then, imidazole (1.7 g, 25 mmol, 2.5 eq.) and TBSCl (1.8 g, 12 mmol, 1.2 eq.) were added. The resulting solution was stirred at ambient temperature for 3 h, after which water and diethylether were added. The layers were separated, and the water layer extracted twice with diethylether. The organic layers were combined, washed with brine and dried over Na₂SO₄, filtered and evaporated till dryness. The residue was purified by column chromatography (100% PET → 2.5% EA/PET) to give **19** (3.1 g, 9.8 mmol) as a colorless oil in 98% yield. ¹H-NMR (300 MHz, CDCl₃) δ: -0.02 (s, 6H, 2 × CH₃), 0.87 (s, 9H, *t*Bu CH₃), 2.77 (t, $J=6.9$ Hz, 2H, Ph-CH₂), 3.78 (t, $J=6.9$ Hz, 2H, CH₂OSi), 7.06–7.10 (m, 2H, H_{phe}), 7.38–7.41 (m, 2H, H_{phe}). Spectral data matched those reported in literature⁴⁸.

*Synthesis of 3-bromophenethoxy(*tert*-butyl)dimethylsilane (20).*



According to the procedure as described for **19**; **3-(4-bromophenyl)-ethanol** (3.0 g, 15 mmol) was transformed into **20** (4.73 g, 15.0 mmol) as a colorless oil in quantitative yield. ¹H-NMR (300 MHz, CDCl₃) δ: -0.03 (s, 6H, Si-(CH₃)₃), 0.87 (s, 9H, *t*Bu), 2.78 (t, $J=6.9$ Hz, 2H, PhCH₂CH₂O), 3.79 (t, $J=6.9$ Hz, 2H, PhCH₂CH₂O), 7.12–7.17 (m, 2H, H_{phe}), 7.32–7.35 (m, 1H, H_{phe}), 7.37–7.38 (m, 1H, H_{phe}). ¹³C-NMR (75 MHz, CDCl₃) δ: -5.32 (2C, Si-CH₃), 18.45 (Si-C-(CH₃)₃), 26.04 (3C, *t*Bu), 39.26 (PhCH₂CH₂O), 64.14 (PhCH₂CH₂O), 122.35, 127.98, 129.32, 129.86, 132.44, 141.89. Spectral data matched those reported in literature³¹.

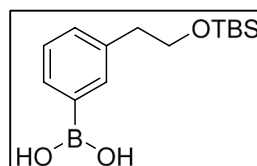
*Synthesis of (4-(2-((*tert*-butyldimethylsilyl)oxy)ethyl)phenyl)boronic acid (21).*



19 (1.9 g, 6.0 mmol, 1 eq.) was dissolved in anhydrous THF (30 mL, 5 mL/mmol SM) in a flame-dried round bottom flask under argon. The resulting solution was cooled to -78 °C. Then, *n*BuLi in hexanes (1.6 M, 4.5 mL, 7.2 mmol, 1.2 eq.) was added dropwise (0.3 mL/min) at -78 °C. After the addition was complete the resulting solution was kept at -78 °C for 1 h, after which B(OMe)₃ (1.0 mL, 9.0 mmol, 1.5 eq.) was added all at once at -78 °C. The solution was stirred at -78 °C for 30 min, after which the cooling bath was removed, and the reaction stirred at ambient temperature for another 2 h. Then, aq. sat. NH₄Cl solution (18 mL, 3 mL/mmol SM) was

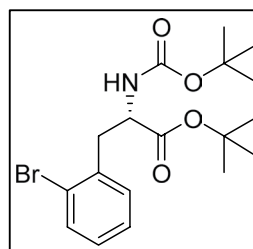
added and stirring continued for 5 min. The organic solvents were removed *in vacuo*, and DCM was added. The pH was adjusted till pH 1 with 3 M aq. HCl solution, and the layers were separated. The water layer was extracted twice with DCM. The organic layers were combined, dried over Na_2SO_4 , filtered and evaporated till dryness. The residue was purified by column chromatography (15 → 50% EA/PET), to give **21** (0.71 g, 2.5 mmol) as a colorless oil in 42% yield. $^1\text{H-NMR}$ (300 MHz, CDCl_3) δ : 0.00 (s, 6H, $2 \times \text{Si-CH}_3$), 0.89 (s, 9H, *t*Bu), 2.91 (t, $J = 6.9$ Hz, 2H, PhCH_2), 3.87 (t, $J = 6.9$ Hz, 2H, $\text{CH}_2\text{-OSi}$), 7.35 (d, $J = 7.8$ Hz, 2H, H_{Phe}), 8.15 (d, $J = 8.1$ Hz, 2H, H_{Phe}). HRMS (ESI): calculated for $\text{C}_{15}\text{H}_{26}\text{BO}_5\text{Si}$ ($[\text{M} + \text{HCOO}]^-$): 325.1648, found: 325.1660. Spectral data matched those reported in literature⁴⁹.

(3-(2-((*tert*-butyldimethylsilyloxy)ethyl)phenyl)boronic acid (**22**).



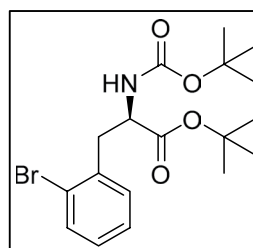
According to the procedure as described for **21**; **20** (1.9 g, 6.0 mmol) was transformed into **22** (0.925 g, 3.30 mmol) as a colorless oil 55% yield. $^1\text{H-NMR}$ (300 MHz, CDCl_3) δ : 0.00 (s, 6H, $2 \times \text{Si-CH}_3$), 0.88 (s, 9H, *t*Bu), 2.95 (t, $J = 7.2$ Hz, 2H, $\text{PhCH}_2\text{CH}_2\text{OTBS}$), 3.80 (t, $J = 6.9$ Hz, 2H, $\text{PhCH}_2\text{CH}_2\text{OTBS}$), 7.20–7.29 (m, 2H, H_{Phe}), 7.30–7.35 (m, 2H, H_{Phe}). Spectral data matched those reported in literature³¹.

tert-butyl (S)-3-(2-bromophenyl)-2-((*tert*-butoxycarbonyl)amino)propanoate (**23** - L-type).

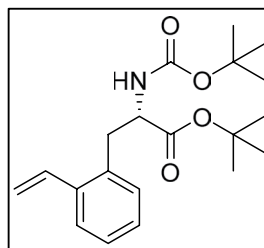


(S)-3-(2-bromophenyl)-2-((*tert*-butoxycarbonyl)amino)propanoic acid (0.69 g, 2.0 mmol, 1 eq.) was dissolved in DCM (20 mL, 10 mL/mmol) under argon. Next, *tert*-butyl 2, 2, 2-trichloroacetimidate (1.3 g, 6.0 mmol, 3 eq.) was added. The resulting solution was stirred at ambient temperature overnight, after which water was added. Then, the layers were separated, and the organic layer was washed with sat. aq. NaHCO_3 solution. The organic layer was dried over Na_2SO_4 , filtered and evaporated. The residue was pre-adsorbed onto Celite® and purified by column chromatography (8% EA/PET); which gave **23** (0.72 g, 1.8 mmol) as an oil that solidified upon standing in 90% yield. $^1\text{H-NMR}$ (300 MHz, CDCl_3) δ : 1.37 (s, 9H, *t*Bu), 1.40 (s, 9H, *t*Bu), 3.06 (dd, $J = 13.8, 8.7$ Hz, 1H, Ph-CH_2), 3.25 (dd, $J = 13.3, 6.0$ Hz, 1H, Ph-CH_2), 4.51–4.59 (m, 1H, CH), 5.06 (d, $J = 7.8$ Hz, 1H, NH), 7.06–7.23 (m, 3H, H_{Phe}), 7.54 (d, $J = 7.8$ Hz, 1H, H_{Phe}). $^{13}\text{C-NMR}$ (75 MHz, CDCl_3) δ : 28.0 (*t*-Bu, CH_3), 28.4 (*t*Bu, CH_3), 39.2 (CH_2), 54.1 (CHNH), 79.7 (*t*Bu, $\text{C-(CH}_3)_3$), 82.2 (*t*Bu, $\text{C-(CH}_3)_3$), 125.2, 127.4, 128.5, 131.5, 133.0, 136.7, 155.1 (C=O_{Boc}), 171.2 ($\text{C=O}_{\text{ester}}$). HRMS (ESI): calculated for $\text{C}_{18}\text{H}_{27}\text{BrNO}_4$ ($[\text{M} + \text{H}]^+$): 400.1118, found: 400.1133. $[\alpha]_{\text{D}}^{20} = +6.03$ (c 0.995, CHCl_3).

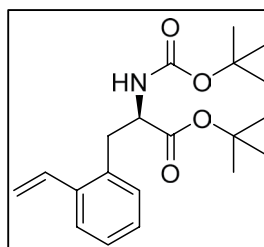
tert-butyl (R)-3-(2-bromophenyl)-2-((*tert*-butoxycarbonyl)amino)propanoate (**24** - D-type).



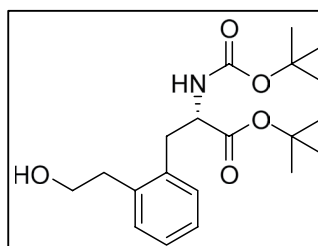
According to the procedure as described for **23**; (R)-3-(2-bromophenyl)-2-((*tert*-butoxycarbonyl)amino)propanoic acid (1.7 g, 5.0 mmol) was transformed into **24** (1.4 g, 3.6 mmol) as a white solid in 72% yield. $^1\text{H-NMR}$ (300 MHz, CDCl_3) δ : 1.37 (s, 9H, *t*Bu), 1.40 (s, 9H, *t*Bu), 3.06 (dd, $J = 14.1, 8.7$ Hz, 1H, Ph-CH_2), 3.25 (dd, $J = 13.8, 6.0$ Hz, 1H, Ph-CH_2), 4.51–4.59 (m, 1H, CH), 5.06 (d, $J = 8.4$ Hz, 1H, NH), 7.07–7.12 (m, 1H, H_{Phe}), 7.19–7.26 (m, 2H, H_{Phe}), 7.54 (d, $J = 8.1$ Hz, 1H, H_{Phe}). $^{13}\text{C-NMR}$ (75 MHz, CDCl_3) δ : 28.0 (*t*Bu, CH_3), 28.4 (*t*Bu, CH_3), 39.2 (CH_2), 54.1 (CHNH), 79.7 (*t*Bu, $\text{C-(CH}_3)_3$), 82.2 (*t*Bu, $\text{C-(CH}_3)_3$), 125.2, 127.4, 128.5, 131.5, 133.0, 136.7, 155.1 (C=O_{Boc}), 171.2 ($\text{C=O}_{\text{ester}}$). HRMS (ESI): calculated for $\text{C}_{18}\text{H}_{27}\text{BrNO}_4$ ($[\text{M} + \text{H}]^+$): 400.1118, found: 400.1132. $[\alpha]_{\text{D}}^{20} = -5.62$ (c 1.46, CHCl_3).

tert-butyl (S)-2-((tert-butoxycarbonyl)amino)-3-(2-vinylphenyl)propanoate (25 – L-type).

23 (0.20 g, 0.50 mmol, 1 eq.), LiCl (0.065 g, 1.5 mmol, 3 eq.) and Pd(Ph₃P)₂Cl₂ (0.018 g, 0.025 mmol, 0.05 eq.) were added to a flame-dried round bottom flask under argon. The air was removed and refilled with argon. This procedure was repeated for three times in total. Then, under argon, anhydrous degassed DMF (2.5 mL, 5 mL/mmol) was added, followed by vinyl-Sn(*n*Bu)₃ (0.19 mL, 0.65 mmol, 1.3 eq.). The resulting mixture was stirred at 70 °C overnight. Then, the mixture was evaporated and re-dissolved in DCM and pre-adsorbed onto Celite®. Then, purification by column chromatography (0 → 10% EA/PET) gave **25** (0.089 g, 0.26 mmol) as an oil in 51% yield. ¹H-NMR (300 MHz, CDCl₃) δ: 1.36 (s, 9H, *t*Bu), 1.40 (s, 9H, *t*Bu), 3.07–3.16 (m, 2H, CH₂), 4.39–4.47 (m, 1H, CHNH), 5.00 (d, *J* = 7.8 Hz, 1H, NH), 5.34 (dd, *J* = 11.1, 1.5 Hz, H_{vinyl}), 5.67 (d, *J* = 17.4 Hz, 1H, H_{vinyl}), 7.04 (dd, *J* = 17.4, 11.1 Hz, 1H, H_{vinyl}), 7.11–7.25 (m, 3H, H_{phe}), 7.50 (dd, *J* = 7.8, 1.8 Hz, 1H, H_{phe}). ¹³C-NMR (75 MHz, CDCl₃) δ: 28.0 (*t*Bu, CH₃), 28.5 (*t*Bu, CH₃), 36.3 (CH₂), 54.9 (CHNH), 79.8 (*t*Bu, C-(CH₃)₃), 82.1 (*t*Bu, C-(CH₃)₃), 116.3 (vinyl-CH₂), 126.1 (vinyl-CH), 127.34, 127.7, 130.8, 134.2, 134.6, 137.6, 155.1 (C=O_{Boc}), 171.3 (C=O_{ester}). HRMS (ESI): calculated for C₂₀H₃₀NO₄ ([M + H]⁺): 348.2169, found: 348.2176. [α]_D²⁰ = +10.71 (c 0.56, CHCl₃).

tert-butyl (R)-2-((tert-butoxycarbonyl)amino)-3-(2-vinylphenyl)propanoate (26 – D-type).

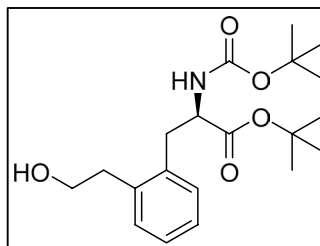
According to the procedure described for **25**; **24** (0.605 g, 1.5 mmol) was transformed into **26** (0.38 g, 1.0 mmol) as a yellowish oil in 67% yield. ¹H-NMR (300 MHz, CDCl₃) δ: 1.35 (s, 9H, *t*Bu), 1.40 (s, 9H, *t*Bu), 3.07–3.16 (m, 2H, CH₂), 4.43 (q, *J* = 7.2 Hz, 1H, CHNH), 5.00 (d, *J* = 7.5 Hz, 1H, NH), 5.34 (dd, *J* = 11.1, 1.5 Hz, 1H, vinyl-H), 5.67 (dd, *J* = 17.4, 1.2 Hz, 1H, H_{vinyl}), 7.04 (dd, *J* = 17.4, 11.1 Hz, 1H, H_{vinyl}), 7.11–7.26 (m, 3H, H_{phe}), 7.50 (dd, *J* = 7.2, 1.8 Hz, 1H, H_{phe}). ¹³C-NMR (75 MHz, CDCl₃) δ: 28.0 (*t*Bu, CH₃), 28.4 (*t*Bu, CH₃), 36.3 (CH₂), 54.9 (CHNH), 79.8 (*t*Bu-C-(CH₃)₃), 82.1 (*t*Bu-C-(CH₃)₃), 116.3 (vinyl-CH₂), 126.0 (vinyl-CH), 127.34, 127.7, 130.8, 134.2, 134.5, 137.6, 155.1 (C=O_{Boc}), 171.3 (C=O_{ester}). HRMS (ESI): calculated for C₂₀H₃₀NO₄ ([M + H]⁺): 348.2169, found: 348.2170. [α]_D²⁰ = -10.21 (c 0.48, CHCl₃).

tert-butyl (S)-2-((tert-butoxycarbonyl)amino)-3-(2-(2-hydroxyethyl)phenyl)propanoate (27 – L-type).

25 (0.33 g, 0.96 mmol, 1 eq.) was dissolved in anhydrous THF (10 mL, 10 mL/mmol SM) under argon. The resulting solution was cooled to 0 °C in an ice-bath. After 5 min, BH₃ in THF (1 M in THF; 0.96 mL, 0.96 mmol, 1 eq.) was added. Then, the ice-bath was removed, and the resulting solution stirred at ambient temperature for 1 h. Then, NaBO₃·H₂O (0.48 g, 4.8 mmol, 5 eq.) was added, followed by water (10 mL, 10 mL/mmol SM). The mixture was vigorously stirred for 2 h. Next, sat. aq. NH₄Cl was added together with EA. The layers were separated, and the water layer extracted twice more with EA. The organic layers were combined, dried over Na₂SO₄, filtered and evaporated till dryness. The residue was purified by column chromatography (0 → 30% EA/PET) to give **27** (0.23 g, 0.64) as a colorless oil in 66% yield. ¹H-NMR (300 MHz, CDCl₃) δ: 1.35 (s, 9H, *t*Bu), 1.38 (s, 9H, *t*Bu), 2.28

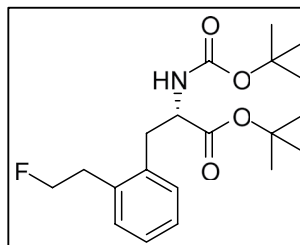
(br. s, 1H, OH), 2.92–3.16 (m, 4H, Ph-CH₂), 3.89 (t, *J* = 6.3 Hz, 2H, CH₂OH), 4.49 (q, *J* = 7.2 Hz, 1H, CHNH), 5.18 (d, *J* = 7.8 Hz, 1H, NH), 7.13–7.22 (m, 4H, H_{Phc}). ¹³C-NMR (75 MHz, CDCl₃) δ: 28.0 (*t*Bu, CH₃), 28.4 (*t*Bu, CH₃), 35.8 (CH₂), 36.8 (CH₂), 54.8 (CHNH), 63.6 (CH₂OH), 80.0 (*t*Bu-C-(CH₃)₃), 82.2 (*t*Bu-C-(CH₃)₃), 126.4, 127.3, 130.0, 131.0, 135.4, 137.6, 155.2 (C=O_{Boc}), 171.4 (C=O_{ester}). HRMS (ESI): calculated for C₂₀H₃₂NO₅ ([M + H]⁺): 366.2275, found: 366.2278. [α]_D²⁰ = +7.17 (c 0.60, CHCl₃).

tert-butyl (*R*)-2-((*tert*-butoxycarbonyl)amino)-3-(2-(2-hydroxyethyl)phenyl)propanoate (**28** - *D*-type).



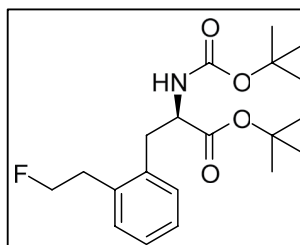
According to the procedure as described for **27**; **26** (0.34 g, 0.99 mmol) was transformed into **28** (0.22 g, 0.60 mmol) as a colorless oil in 61% yield. ¹H-NMR (300 MHz, CDCl₃) δ: 1.35 (s, 9H, *t*Bu), 1.38 (s, 9H, *t*Bu), 2.33 (br. s, 1H, OH), 2.95 (dd, *J* = 13.8, 6.6 Hz, 1H, PhCH₂), 2.95 (dd, *J* = 13.8, 8.1 Hz, 2H, PhCH₂), 3.13 (dd, *J* = 13.8, 6.9 Hz, 1H, PhCH₂), 3.90 (t, *J* = 6.3 Hz, 2H, CH₂OH), 4.45–4.53 (m, 1H, CHNH), 5.17 (d, *J* = 8.1 Hz, 1H, NH), 7.12–7.23 (m, 4H, H_{Phc}). ¹³C-NMR (75 MHz, CDCl₃) δ: 28.0 (*t*Bu, CH₃), 28.4 (*t*Bu, CH₃), 35.8 (CH₂), 37.0 (CH₂), 54.8 (CHNH), 63.6 (CH₂OH), 80.0 (*t*Bu-C-(CH₃)₃), 82.3 (*t*Bu-C-(CH₃)₃), 126.5, 127.3, 130.0, 131.1, 135.5, 137.6, 155.2 (C=O_{Boc}), 171.4 (C=O_{ester}). HRMS (ESI): calculated for C₂₀H₃₂NO₅ ([M + H]⁺): 366.2275, found: 366.2260. [α]_D²⁰ = -6.67 (c 0.48, CHCl₃).

tert-butyl (*S*)-2-((*tert*-butoxycarbonyl)amino)-3-(2-(2-fluoroethyl)phenyl)propanoate (**29** - *L*-type).



27 (0.090 g, 0.25 mmol, 1 eq.) was dissolved in anhydrous DCM (2.5 mL, 10 mL/mmol SM) under argon and cooled in an ice bath at 0 °C. Then, DAST (0.10 mL, 0.74 mmol, 3 eq.) was added dropwise and the mixture was stirred at ambient temperature for approximately 3–4 h. Then, the mixture was cooled to 0 °C in an ice bath and aq. sat. NaHCO₃ solution was added dropwise. After the gas evolution ceased, the mixture was transferred into a separatory funnel and more sat. aq. NaHCO₃ solution was added. The layers were separated, and the water layer extracted twice more with DCM. The organic layers were combined, dried over Na₂SO₄, filtered and evaporated till dryness. The residue was purified by column chromatography (0 → 12% EA/PET) to give **29** (0.041 g, 0.11 mmol) as a yellowish oil in 45% yield. ¹H-NMR (300 MHz, CDCl₃) δ: 1.37 (s, 9H, *t*Bu), 1.40 (s, 9H, *t*Bu), 3.01–3.17 (m, 4H, PhCH₂), 4.37–4.45 (m, 1H, PhCHNH), 4.63 (dt, *J* = 46.8, 6.9 Hz, 2H, CH₂F), 5.03 (d, *J* = 8.4 Hz, 1H, NH), 7.11–7.22 (m, 4H, H_{Phc}). ¹⁹F-NMR (282 MHz, CDCl₃) δ: -215.01 – -214.52 (m). ¹³C-NMR (75 MHz, CDCl₃) δ: 28.0 (*t*Bu, CH₃), 28.4 (*t*Bu, CH₃), 33.6 (d, *J* = 20.6 Hz, 1C, PhCH₂CH₂F), 36.1 (PhCH₂), 54.9 (CHNH), 79.9 (*t*Bu-C-(CH₃)₃), 82.2 (*t*Bu-C-(CH₃)₃), 84.0 (d, *J* = 169.4 Hz, 1C, PhCH₂CH₂F), 126.9, 127.3, 130.1, 130.8, 135.3 (Ph-C-CH₂CHNH), 135.9 (d, *J* = 6.9 Hz, 1C, Ph-C-CH₂CH₂F), 155.2 (C=O_{Boc}), 171.4 (C=O_{ester}). HRMS (ESI): calculated for C₂₀H₃₁FNO₄ ([M + H]⁺): 368.2232, found: 368.2220. [α]_D²⁰ = +21.87 (c 0.48, CHCl₃).

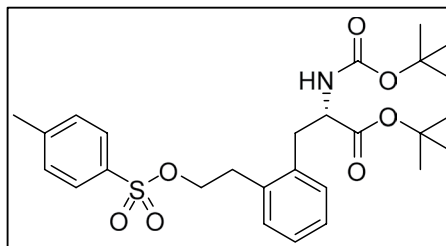
tert-butyl (*R*)-2-((*tert*-butoxycarbonyl)amino)-3-(2-(2-fluoroethyl)phenyl)propanoate (**30** - *D*-type).



According to the procedure as described for **29**; **28** (0.185 g, 0.506 mmol) was transformed into **30** (0.101 g, 0.273 mmol) as a colorless oil in 54% yield. ¹H-NMR (300 MHz, CDCl₃) δ: 1.36 (s, 9H, *t*Bu), 1.39 (s, 9H, *t*Bu),

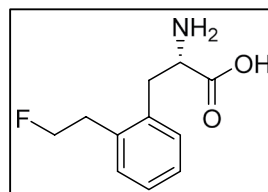
2.97–3.19 (m, 4H, Ph-CH₂), 4.37–4.44 (m, 1H, PhCHNH), 4.62 (dt, $J = 47.1, 6.9$ Hz, 2H, CH₂F), 5.05 (d, $J = 8.4$ Hz, 1H, NH), 7.15–7.23 (m, 4H, H_{Ph}). ¹⁹F-NMR (282 MHz, CDCl₃) δ : –215.02 – –214.53 (m). ¹³C-NMR (75 MHz, CDCl₃) δ : 28.0 (tBu, CH₃), 28.4 (tBu, CH₃), 33.6 (d, $J = 20.6$ Hz, 1C, PhCH₂CH₂F), 36.1 (PhCH₂), 54.9 (CHNH), 79.8 (tBu-C-(CH₃)₃), 82.2 (tBu-C-(CH₃)₃), 83.9 (d, $J = 168.3$ Hz, 1C, PhCH₂CH₂F), 126.9, 127.3, 130.0, 130.7, 135.3 (Ph-C-CH₂CHNH), 135.9 (d, $J = 5.7$ Hz, 1C, Ph-C-CH₂CH₂F), 155.2 (C=O_{Boc}), 171.3 (C=O_{ester}). HRMS (ESI): calculated for C₂₀H₃₂NO₅ ([M + H]⁺): 366.2275, found: 366.2260. $[\alpha]_D^{20} = -22.40$ (c 0.50, CHCl₃).

tert-butyl (S)-2-((*tert*-butoxycarbonyl)amino)-3-(2-(2-(tosyloxy)ethyl)phenyl)propanoate (31 - L-type).



27 (0.22 g, 0.60 mmol, 1 eq.) was dissolved in anhydrous DCM (6.0 mL, 10 mL/mmol SM), after which Et₃N (0.252 mL, 1.81 mmol, 3 eq.) was added. Then, a catalytic amount of DMAP followed by tosylchloride (0.138 g, 0.722 mmol, 1.2 eq.) were added, and the resulting solution stirred at ambient temperature for 2 h. Next, water was added, and the layers separated. The water layer was extracted twice with DCM. The organic layers were combined, dried over Na₂SO₄, filtered and evaporated. The residue was purified by column chromatography (0 → 20% EA/PET) to give **31** (0.175 g, 0.337 mmol) as a colorless oil in 56% yield. ¹H-NMR (300 MHz, CDCl₃) δ : 1.35 (s, 9H, tBu), 1.39 (s, 9H, tBu), 2.43 (s, 3H, CH₃), 2.87–3.12 (m, 4H, PhCH₂), 4.12–4.24 (m, 2H, CH₂OTs), 4.30–4.37 (m, 1H, CHNH), 4.99 (d, $J = 8.4$ Hz, 1H, NH), 7.05–7.16 (m, 4H, H_{Ph}), 7.26–7.30 (m, 2H, H_{Ph-Ts}), 7.68–7.72 (m, 2H, H_{Ph-Ts}). ¹³C-NMR (75 MHz, CDCl₃) δ : 21.8 (CH₃), 28.0 (tBu, CH₃), 28.4 (tBu, CH₃), 32.1 (PhCH₂CH₂OTs), 36.0 (PhCH₂CH), 54.8 (PhCH₂CH), 70.3 (PhCH₂CH₂OTs), 79.9 (tBu-C-(CH₃)₃), 82.3 (tBu-C-(CH₃)₃), 127.1, 127.4, 128.0, 129.95, 130.04, 130.8, 133.2, 135.0, 135.3, 144.8, 155.1 (C=O_{Boc}), 171.21 (C=O_{ester}). HRMS (ESI): calculated for C₂₇H₂₈NO₇S ([M + H]⁺): 520.2363, found: 520.2375. $[\alpha]_D^{20} = +11.06$ (c 1.09, CHCl₃).

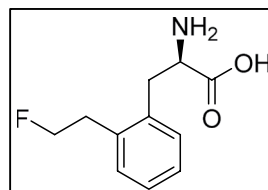
(S)-2-amino-3-(2-(2-fluoroethyl)phenyl)propanoic acid (32 - L-type, 2-FELP).



29 (0.090 g, 0.25 mmol) was dissolved in DCM (3.0 mL) after which TFA (3.0 mL) was added. The resulting solution was stirred at ambient temperature for approximately 5 hours, after which it was evaporated till dryness. Next, the residue was co-evaporated with MeOH three times. Then, the residue was dissolved in ~2 mL of MeOH and the pH was adjusted to pH 6–7, with diluted aq. NH₃ solution, after which a white precipitate formed. The mixture was refrigerated overnight, and then the liquid was removed via pipette aspiration. The remaining solid was washed thrice with a minimal amount of ice-cold MeOH and dried under high vacuum to give **2-FELP** (0.012 g, 0.057 mmol) as a white powder in 23% yield. ¹H-NMR (300 MHz, D₂O) δ : 3.10 (dd, $J = 14.7, 9.0$ Hz, 1H, PhCH₂CH), 3.15 (dt, $J = 26.4, 6.0$ Hz, 2H, PhCH₂CH₂F), 3.43 (dd, $J = 14.7, 6.0$ Hz, 1H, PhCH₂CH), 3.95 (dd, $J = 9.0, 6.0$ Hz, 1H, PhCH₂CH), 4.77 (dt, $J = 47.4, 6.0$ Hz, 2H, PhCH₂CH₂F), 7.31–7.43 (m, 4H, H_{Ph}). ¹⁹F-NMR (282 MHz, D₂O) δ : –218.58 (tt, $J = 46.8, 26.5$ Hz, 1F). ¹³C-NMR (75 MHz, D₂O) δ : 32.4 (d, $J = 19.4$ Hz, 1C, PhCH₂CH₂F), 33.5 (PhCH₂CH), 55.6 (PhCH₂CH), 85.0 (d, $J = 161.4$ Hz, 1C, PhCH₂CH₂F), 127.3, 128.0, 130.3, 130.4, 134.0, 136.5 (d, $J = 4.6$ Hz, 1C, Ph-C-CH₂CH₂F), 173.9 (C=O). HRMS (ESI): calculated for C₁₁H₁₅FNO₂ ([M + H]⁺): 212.1081, found: 212.1078.

Chiral HPLC: Astec® Chirobiotic T column (5 μ m, 125 mm \times 4.6), EtOH(abs.)/H₂O (80/20), retention time: 4.01 min, ee: 90.4%.

(R)-2-amino-3-(2-(2-fluoroethyl)phenyl)propanoic acid.HCl salt (33 - D-type, 2-FEDP).



30 (0.090 g, 0.25 mmol) was dissolved in DCM (3.0 mL) after which TFA (3.0 mL) was added. The resulting solution was stirred at ambient temperature for approximately 5 hours, after which it was evaporated till dryness. Next, the residue was co-evaporated with MeOH three times. Then, the residue was dissolved in ~2 mL of MeOH and the pH was adjusted to pH 6–7, with diluted aq. NH₃ solution, after which a white precipitate formed. The mixture was refrigerated overnight, and then the liquid was removed via pipette aspiration. The remaining solid was washed once with a minimal amount of ice-cold MeOH and re-dissolved in MeOH. Then, 1.25 M HCl in MeOH was added and the mixture evaporated till dryness. The residue was dissolved in water and lyophilized, which gave rise to **34** (0.030 g, 0.12 mmol) as a white, amorphous powder in 49% yield. ¹H-NMR (300 MHz, D₂O) δ: 3.14 (dt, *J* = 26.7, 6.0 Hz, 2H, PhCH₂CH₂F), 3.13–3.21 (m, 1H, PhCH₂CH), 3.48 (dd, *J* = 14.7, 6.3 Hz, 1H, PhCH₂CH), 4.13–4.19 (m, 1H, PhCH₂CH), 4.77 (dt, *J* = 47.1, 6.0 Hz, 2H, PhCH₂CH₂F), 7.31–7.44 (m, 4H, H_{Ph}). ¹⁹F-NMR (282 MHz, D₂O) δ: –216.10 (tt, *J* = 46.8, 26.5 Hz, 1 F). ¹³C-NMR (75 MHz, D₂O) δ: 32.35 (d, *J* = 19.4 Hz, 1C, PhCH₂CH₂F), 33.1 (PhCH₂CH), 54.4 (PhCH₂CH), 85.0 (d, *J* = 161.4 Hz, 1C, PhCH₂CH₂F), 127.4, 128.2, 130.3, 130.4, 133.4, 136.6 (d, *J* = 4.6 Hz, 1C, Ph-C-CH₂CH₂F), 172.4 (C=O). HRMS (ESI): calculated for C₁₁H₁₅FNO₂ ([M + H]⁺): 212.1081, found: 212.1085.

Chiral HPLC Astec® Chirobiotic T column (5 μm, 125 mm × 4.6), EtOH(abs.)/H₂O (80/20), retention time: 5.21 min, *ee*: 75.2%.

In vitro experiments. *General information.* The F98 GB cell line was obtained from ATCC and cultivated as described previously¹¹. Cells were tested and authenticated by the provider and were cultured for maximum ten weeks after retrieval from liquid nitrogen.

LAT1 expression was determined using flow cytometry. F98 cells (100,000 per well) were surface stained with a monoclonal antibody against LAT1 (PE-conjugated, Santa Cruz biotechnology, Heidelberg, Germany), which acts as a negative control. As described by De Munter *et al.*⁵⁰, cells were subsequently fixed, permeabilized and submitted for intracellular staining with the same PE conjugated monoclonal antibody against LAT1. Flow cytometric analysis was performed using the LSR II (BD Biosciences).

In vitro experiments were carried out in 24-well-plates (VWR, US), using at least three wells for each data-point. The cells were seeded 24 h prior to the experiment at 200,000 cells/well. Influx of radiolabeled AA was studied in a Na⁺ containing buffer (HEPES+ buffer: pH 7.4; 100 mM NaCl (Sigma Aldrich, Belgium), 2 mM KCl (Sigma Aldrich, Belgium), 1 mM MgCl₂ (VWR, US), 1 mM CaCl₂ (VWR, US), 10 mM Hepes (Sigma Aldrich, Belgium), 5 mM Tris (VWR, US), 1 g/L glucose (VWR, US) and 1 g/L Bovine Serum Albumin (Sigma Aldrich, Belgium)) and/or a Na⁺ free buffer (HEPES- buffer: pH 7.4; 100 mM Choline-Cl (Sigma Aldrich, Belgium), 2 mM KCl, 1 mM MgCl₂, 1 mM CaCl₂, 10 mM Hepes, 5 mM Tris, 1 g/L glucose and 1 g/L Bovine Serum Albumin). The culture medium was removed, and cells were washed twice with 1 mL HEPES+/HEPES- buffer. Dosing solutions were prepared by supplementing the washing buffer with either 11 kBq [2, 3, 4, 5, 6-³H]-L-phenylalanine (Perkin Elmer, Massachusetts, USA)/mL or with 37 kBq of the [¹⁸F]-labelled AA. The incubation process was terminated by cooling the plates on ice and adding 1 mL 1% BSA ice-cold PBS. Cells were washed twice with 2 mL ice-cold PBS. Subsequently, cells were lysed with 250 μL 0.1 M NaOH (VWR, US) and radioactivity stemming from the [¹⁸F]-isotope was counted by subjecting 150 μL of this solution to an automated gamma-counter (Cobra-inspector 5003, Canberra Packard, Meriden, CT, USA). [³H] samples (150 μL) were transferred to a scintillation bottle (Perkin Elmer, Massachusetts, USA) containing 5 mL of scintillation liquid (Ultima Gold, Perkin Elmer, Massachusetts, USA) and counted using an automated scintillation counter (TriCarb 2900 TR; Perkin Elmer, Massachusetts, USA). Of each well, 25 μL was subjected to a BCA assay (ThermoFisher Scientific) to determine protein content.

Concentration dependency using [2, 3, 4, 5, 6-³H]-L-phenylalanine. Non-linear curve fitting was performed to determine the Michaelis-Menten kinetics using Graphpad Prism v5.01 (Graphpad software, San Diego, CA, USA). These were employed to study the potential inhibition of the AA analogue towards the [³H]-L-Phe/L-Phe couple with varying concentrations (0.01 to 0.5 mM) at 1 min uptake (V₀ conditions). The apparent K_m and corresponding K_i values were calculated according to the formula:

$$K_i = [I] / ((K_{m,app} / K_m) - 1)$$

where [I] is the inhibitor concentration (i.e. the fluorinated AA), K_m is the Michaelis-Menten constant of the substrate (i.e. ³H-L-Phe/L-Phe) and K_{m,app} is the apparent value of K_m for substrate transport in the presence of the inhibitor.

Radiochemical synthesis and purification. The radiofluorinated AA analogues, [¹⁸F]FET and 2-(2-[¹⁸F]fluoroethyl)-L-phenylalanine (2-[¹⁸F]FELP) were prepared on a Synthra RN plus module (Synthra GmbH, Hamburg, Germany) with an integrated semi-preparative HPLC, using identical reaction and purification conditions for both tracers, based on the method described by Bourdier *et al.*⁵¹ (depicted in Supplementary Fig. 1). The precursor solution for radiolabeling was prepared by dissolving 6 mg tert-butyl (S)-3-(4-(2-(tosyloxy)ethoxy)phenyl)-2-(tritylamino)propanoate (ABX, Germany) or 9 mg tert-butyl (S)-2-((tert-butoxycarbonyl)amino)-3-(2-(2-(tosyloxy)ethyl)phenyl)propanoate in 1 mL acetonitrile (Sigma Aldrich, Belgium). The precursor solution was added to a dried [¹⁸F]F⁻/Kryptofix®222/K⁺ complex, heated at 100 °C for 15 min. Subsequently, deprotection was performed by adding 2 M HCl (1 mL) for 15 min. The solution was then neutralized with 4 M NaOH, followed by adding 0.10 M NH₄OAc. HPLC purification was performed using a RP symmetry Prep C18 column (5 μm, 10 × 250 mm, Machery-Nagel, Duren, Germany), a 0.01 M NH₄OAc buffer in ethanol/water 5/95 (V/V) mobile phase, and a flow rate of 5 mL/min. The fraction containing purified [¹⁸F]FET or 2-[¹⁸F]FELP eluted at approximately 12 min and 15 min respectively (depicted in Supplementary Figs 2 and 3 for [¹⁸F]FELP), and was collected

for 2 minutes. This procedure yielded in 3.32 ± 1.16 GBq [^{18}F]FET or 3.01 ± 0.97 MBq 2-[^{18}F]FELP. Quality control of the final formulation was performed by radio-TLC using Polygram TLC stripes (Macherey-Nagel, Germany), a mobile phase consisting of ACN/H₂O 95/5 (V/V), and miniGITA (Raytest, Germany) analysis software. Radiochemical purities of $\geq 95\%$ were obtained for [^{18}F]FET and for 2-[^{18}F]FELP. Chiral purity of [^{18}F]FELP was assessed as described for the unlabelled amino acid.

1 MBq of 2-[^{18}F]FELP or 2-[^{18}F]FET was added to a 1:1 v:v mixture of MilliQ water and n-octanol in a test tube. After vortexing and centrifugation (10 min; 1100 g) of the samples, aliquots were taken from each layer and counted separately in a NaI (TI) scintillation counter (Capintec; Ramsey, NJ, USA). The partition coefficient was calculated using the ratio of activity detected in n-octanol and in the aqueous layer to obtain the $\log P_{\text{oct}}$ value.

Concentration and time dependency using 2-[^{18}F]FELP or [^{18}F]FET. Concentration dependency was measured at V_0 conditions with concentrations of the AA varying from 0.01 to 0.5 mM. The data were fitted to the Michaelis-Menten model and the K_m was calculated.

The cells were incubated for times ranging from 1–60 min in 250 μL of HEPES+ buffer supplemented with 37 kBq of 2-[^{18}F]FELP or [^{18}F]FET.

To determine the selectivity of the LAT1 transporter for the fluor-18 labelled AA, the *in vitro* uptake was studied in the presence of Na⁺-rich or Na⁺-free buffer (HEPES+/- buffer), 8 mM of the system L and b^{0,+} inhibitor 2-aminobicycloheptane-2-carboxylic acid (BCH) (Sigma Aldrich, Belgium), 8 mM of the system A inhibitor methylaminoisobutyric acid (MeAiB) (Sigma Aldrich, Belgium) or 5 mM of the LAT1 specific inhibitor JPH-203 (ARK Pharm, USA). The uptake studies supplemented with the transporter specific inhibitors were carried out in HEPES+ buffer.

In vivo experiments. The study was performed in accordance with the appropriate guidelines and regulations and approved by the Ghent University Ethical Committee on animal experiments (ECD15/39). The GB F98 rat model was developed as described by Bolcaen *et al.*¹¹. Six female NIH-Foxn1^{tmu} rats were inoculated with $\pm 20,000$ F98 tumor cells in the right frontal lobe. The rats were anesthetized with ketamine/xylazine (4/3; 0.13 ml/100 g) and were kept separately post-inoculation (p.i.).

Tumor growth was evaluated 8 days p.i. using MRI (7T PharmaScan 70/16, Bruker BioSpin, Ettlingen, Germany). The rats were anesthetized with 2% isoflurane mixed with oxygen administered at a flow rate of 0.3 L/min. After fixation, a heated blanket was placed on the animal. A rat brain surface coil (Rapid Biomedical, Rimpär, Germany) was placed around the head, after which the holder was positioned in a 72 mm rat whole body transmitter coil (Rapid Biomedical, Rimpär, Germany). After performing a localizer scan, a T2-weighted spin-echo scan (TR/TE 3661/37.1 ms, 109 μm isotropic in plane resolution, 4 averages, TA 9'45'') was obtained. If a tumor was visible, a gadolinium-containing contrast agent (Dotarem, Guerbet, France; 0.4 mL/kg) was injected intravenously through a 30-Gauge needle connected to a 60 cm long PE tube into the tail vein. A contrast-enhanced T1-weighted spin-echo sequence (TR/TE 1539/9.7 ms, 117 μm isotropic in plane resolution, 3 averages, TA 4'15'') was performed 15 min post injection of the contrast agent.

When the presence of a tumor was confirmed, additional contrast-enhanced T1-weighted spin-echo scans were obtained, as above-mentioned. Post-MRI dynamic PET scans were acquired using 2-[^{18}F]FELP, [^{18}F]FET and [^{18}F]FDG on three consecutive days (day 13, 14 and 15 p.i.). The total acquisition time was 120 min for both dynamic AA PET scans and 60 min for the dynamic [^{18}F]FDG PET ([^{18}F]FDG_{early}). In addition, a static 30 min [^{18}F]FDG PET was acquired 240 min post-injection ([^{18}F]FDG_{late}).

All PET scans were reconstructed into a $200 \times 200 \times 128$ matrix by a 3D Maximum Likelihood Expectation Maximization (MLEM) algorithm (LabPET Version 1.12.1, TriFoil Imaging[®], Northridge CA) using 50 iterations and a voxel size of $0.5 \times 0.5 \times 0.59675$ mm. The dynamically acquired PET data were reconstructed into different time frames. Time frames were 6×20 s, 3×1 min, 3×5 min and 2×20 min for [^{18}F]-FDG scans and 6×20 s, 3×1 min, 3×5 min and 5×20 min for the AA PET.

Rigid body PET-MRI co-registration was done using PMOD (PMOD technologies[®], Zürich, Switzerland) and volumes of interest (VOI) were manually drawn, including the contrast-enhanced region on T1-weighted MRI. Cubic VOIs of $2 \times 2 \times 2$ mm located in the contralateral region were used as a reference. Tracer uptake in the VOI at each time frame was converted to a standard uptake value (SUV) according to the following formula:

$$\text{SUV} = (\text{Radioactivity in VOI/injected activity}) \times \text{body weight}$$

Injected activity was corrected for radioactive decay and residual activity in the syringe. Standardized uptake values (SUV_{mean} and SUV_{max}) and tumor-to-background ratios (TBR_{mean} and TBR_{max}) were calculated.

Data analysis. All data are expressed as means \pm SD. All curves were constructed using GraphPad Prism 5.0 (GraphPad Software, San Diego, CA, USA). Where applicable, statistical analysis was performed using the Mann-Whitney U test. A probability value of $p < 0.05$ was considered statistically significant.

Data Availability

All data generated or analyzed during this study are included in this published article (and its supplementary information file).

References

- Gulyás, B. & Halldin, C. New PET radiopharmaceuticals beyond FDG for brain tumor imaging. *Q. J. Nucl. Med. Mol. Imaging* **56**, 173–190 (2012).
- Langen, K. J., Galldiks, N., Hattingen, E. & Shah, N. J. Advances in neuro-oncology imaging. *Nat. Rev. Neurol.* **13**, 279–289 (2017).

3. Galldiks, N. & Langen, K. J. Applications of PET imaging of neurological tumors with radiolabeled amino acids. *Q. J. Nucl. Med. Mol. Imaging* **59**, 70–82 (2015).
4. Lopci, E. *et al.* PET radiopharmaceuticals for imaging of tumor hypoxia: a review of the evidence. *Am J Nucl Med Mol Imaging* **4**, 365–84 (2014).
5. Bouhlef, A. *et al.* Effect of α -methyl versus α -hydrogen substitution on brain availability and tumor imaging properties of heptanoic [F-18]fluoroalkyl amino acids for positron emission tomography (PET). *J. Med. Chem.* **59**, 3515–3531 (2016).
6. McConathy, J. *et al.* Radiohalogenated nonnatural amino acids as PET and SPECT tumor imaging agents. *Med. Res. Rev.* **32**, 868–905 (2012).
7. Laverman, P., Boerman, O. C., Corstens, F. H. M. & Oyen, W. J. G. Fluorinated amino acids for tumour imaging with positron emission tomography. *Eur. J. Nucl. Med. Mol. Imaging* **29**, 681–90 (2002).
8. Fotiadis, D., Kanai, Y. & Palacin, M. The SLC3 and SLC7 families of amino acid transporters. *Mol. Aspects Med.* **34**, 139–58 (2013).
9. Fuchs, B. C. & Bode, B. P. Amino acid transporters ASCT2 and LAT1 in cancer: partners in crime? *Semin. Cancer Biol.* **15**, 254–66 (2005).
10. Feral, C. C. *et al.* 18F-fluorodihydroxyphenylalanine PET/CT in pheochromocytoma and paraganglioma: relation to genotype and amino acid transport system L. *Eur. J. Nucl. Med. Mol. Imaging* **44**, 812–821 (2017).
11. Bolcaen, J. *et al.* (18F)-fluoromethylcholine (FCho), (18F)-fluoroethyltyrosine (FET), and (18F)-fluorodeoxyglucose (FDG) for the discrimination between high-grade glioma and radiation necrosis in rats: A PET study. *Nucl. Med. Biol.*, <https://doi.org/10.1016/j.nucmedbio.2014.07.006> (2014).
12. Sun, A., Liu, X. & Tang, G. Carbon-11 and Fluorine-18 labeled amino acid tracers for positron emission tomography imaging of tumors. *Front. Chem.* **5**, 1–16 (2018).
13. Lahoutte, T. *et al.* SPECT and PET amino acid tracer influx via system L (h4F2 hc - hLAT1) and its transstimulation. *J. Nucl. Med.* **45**, 1591–1596 (2004).
14. Hutterer, M. *et al.* FET PET: a valuable diagnostic tool in neuro-oncology, but not all that glitters is glioma. *Neuro. Oncol.* **15**, 341–351 (2013).
15. Floeth, F. W. *et al.* 18F-FET PET differentiation of ring-enhancing brain lesions. *J. Nucl. Med.* **47**, 776–82 (2006).
16. Deloar, H. M. *et al.* Estimation of internal absorbed dose using whole-body positron emission tomography. *Eur. J. Nucl. Med.* **25** (1998).
17. Pauleit, D. *et al.* Whole-body distribution and dosimetry of O-(2-[18F]fluoroethyl)-L-tyrosine. *Eur. J. Nucl. Med. Mol. Imaging* **30**, 519–524 (2003).
18. McConathy, J. & Goodman, M. Non natural aminoacids for tumor imaging using PET and SPECT. *Cancer Metastasis Rev* **27**, 555–573 (2008).
19. Wiriyasermkul, P. *et al.* Transport of 3-fluoro-L-alpha-methyl-tyrosine by tumor-upregulated L-type amino acid transporter 1: a cause of the tumor uptake in PET. *J. Nucl. Med.* **53**, 1253–1261 (2012).
20. Ono, M. *et al.* Assessment of amino acid/drug transporters for renal transport of [18F]fluciclovine (anti-[18F]FACBC) *in vitro*. *Int. J. Mol. Sci.* **17** (2016).
21. Chiotellis, A. *et al.* Synthesis, radiolabeling, and biological evaluation of 5-hydroxy-2-[18F]fluoroalkyl-tryptophan analogues as potential PET radiotracers for tumor imaging. *J. Med. Chem.* **59**, 5324–5340 (2016).
22. Zha, Z., Ploessl, K., Lieberman, B. P., Wang, L. & Kung, H. F. Alanine and glycine conjugates of [18F](2S,4R)4-fluoroglutamine for tumor imaging. *Nucl. Med. Biol.* **60**, 19–28 (2018).
23. Ohshima, Y. *et al.* Biological evaluation of 3-[(18F)fluoro- α -methyl-D-tyrosine (D-[(18F)F]FAMT) as a novel amino acid tracer for positron emission tomography. *Ann. Nucl. Med.* **27**, 314–24 (2013).
24. Horiguchi, K. *et al.* Clinical value of fluorine-18 α -methyltyrosine PET in patients with gliomas: comparison with fluorine-18 fluorodeoxyglucose PET. *EJNMMI Res.* **7** (2017).
25. Wang, L., Qu, W., Lieberman, B. P., Plössl, K. & Kung, H. F. Synthesis, uptake mechanism characterization and biological evaluation of (18F) labeled fluoroalkyl phenylalanine analogs as potential PET imaging agents. *Nucl. Med. Biol.* **38**, 53–62 (2011).
26. Kersemans, V. *et al.* 123I/125I-labelled 2-iodo-L-phenylalanine and 2-iodo-D-phenylalanine: comparative uptake in various tumour types and biodistribution in mice. *Eur. J. Nucl. Med. Mol. Imaging* **33**, 919–27 (2006).
27. Bauwens, M. *et al.* Comparison of the uptake of [123I/125I]-2-iodo-D-tyrosine and [123I/125I]-2-iodo-L-tyrosine in R1M rhabdomyosarcoma cells *in vitro* and in R1M tumor-bearing Wag/Rij rats *in vivo*. *Nucl. Med. Biol.* **33**, 735–41 (2006).
28. Wang, L., Lieberman, B. P., Plössl, K., Qu, W. & Kung, H. F. Synthesis and comparative biological evaluation of L- and D-isomers of 18F-labeled fluoroalkyl phenylalanine derivatives as tumor imaging agents. *Nucl. Med. Biol.* **38**, 301–312 (2011).
29. Heckel, T., Bröer, A., Wiesinger, H., Lang, F. & Bröer, S. Asymmetry of glutamine transporters in cultured neural cells. *Neurochem. Int.* **43**, 289–298 (2003).
30. Wang, J. *et al.* Nickel-catalyzed cross-coupling of redox-active esters with boronic acids. *Angew. Chemie - Int. Ed.* **55**, 9676–9679 (2016).
31. Alonso, R., Caballero, A., Campos, P. J. & Rodríguez, M. A. Photochemistry of acyloximes: Synthesis of heterocycles and natural products. *Tetrahedron* **66**, 8828–8831 (2010).
32. Sleveland, D. & Bjørsvik, H. R. Synthesis of phenylboronic acids in continuous flow by means of a multijet oscillating disc reactor system operating at cryogenic temperatures. *Org. Process Res. Dev.* **16**, 1121–1130 (2012).
33. Drugbank. L-Phenylalanine. Available at: <https://www.drugbank.ca/drugs/DB00120>. (Accessed: 15th March 2018).
34. Barth, R. F. & Kaur, B. Rat brain tumor models in experimental neuro-oncology: The C6, 9L, T9, RG2, F98, BT4C, RT-2 and CNS-1 gliomas. *J. Neurooncol.* **94**, 299–312 (2009).
35. Galldiks, N., Law, I., Pope, W. B., Arbizu, J. & Langen, K. J. The use of amino acid PET and conventional MRI for monitoring of brain tumor therapy. *NeuroImage Clin.* **13**, 386–394 (2017).
36. Chien, H.-C. *et al.* Reevaluating the substrate specificity of the L-type amino acid transporter (LAT1). *J. Med. Chem.* **61**, 7358–7373 (2018).
37. Peura, L. *et al.* Large amino acid transporter 1 (LAT1) prodrugs of valproic acid: New prodrug design ideas for central nervous system delivery. *Mol. Pharm.* **8**, 1857–1866 (2011).
38. Nicolaides, D. N., Gautam, D. R., Litinas, K. E., Dimitra, J. & Kontogiorgis, C. A. Synthesis and biological evaluation of O-[3-18F-fluoropropyl]- α -methyl tyrosine in mesothelioma-bearing rodents. *Biomed Res. Int.* **1**–9 (2013).
39. Wang, Q. & Holst, J. L-type amino acid transport and cancer: Targeting the mTORC1 pathway to inhibit neoplasia. *Am. J. Cancer Res.* **5**, 1281–1294 (2015).
40. Langen, K. J. *et al.* Comparison of fluorotyrosines and methionine uptake in F98 rat gliomas. *Nucl. Med. Biol.* **30**, 501–508 (2003).
41. Habermeyer, A. *et al.* System l amino acid transporter LAT1 accumulates O-(2-fluoroethyl)-L-tyrosine (FET). *Amino Acids* **47**, 335–344 (2015).
42. Zhen, H. *et al.* Relation of 4F2hc expression to pathological grade proliferation and angiogenesis in human brain gliomas. *BMC Clin. Pathol.* **12**, 1161–1164 (2012).
43. Dunet, V., Pomoni, A., Hottinger, A., Nicod-Lalonde, M. & Prior, J. O. Performance of 18F-FET versus 18F-FDG-PET for the diagnosis and grading of brain tumors: systematic review and meta-analysis. *Neuro. Oncol.* **18**, 426–34 (2016).
44. Van Winkle, L. J. *et al.* *Biomembrane Transport* (Academic Press, 1999).
45. Chen, W. Clinical applications of PET in brain tumors. *J. Nucl. Med.* **48**, 1468–81 (2007).
46. Galldiks, N. *et al.* Role of O-(2-18F-Fluoroethyl)-L-Tyrosine PET as a diagnostic tool for detection of malignant progression in patients with low-grade glioma. *J. Nucl. Med.* **54**, 2046–2054 (2013).
47. Huszthy, P. C. *et al.* *In vivo* models of primary brain tumors: Pitfalls and Perspectives. *Neuro. Oncol.* **14**, 979–993 (2012).
48. Wegner, J. *et al.* A total synthesis of millingtonineA. *Org. Lett.* **14**, 696–699 (2012).

49. Santora, V. J. *et al.* Heterocyclic biphenyl compounds as modulators of the histamine H₃-receptor useful for the treatment of disorders related thereto and their preparation. WO2009058300A1 (2009).
50. De Munter, S. *et al.* Nanobody based dual specific CARs. *Int. J. Mol. Sci.* **19**, 1–11 (2018).
51. Bourdier, T. *et al.* Fully automated one-pot radiosynthesis of O-(2-[¹⁸F]fluoroethyl)-L-tyrosine on the TracerLab FXFN module. *Nucl. Med. Biol.* **38**, 645–651 (2011).

Acknowledgements

F.H. thanks the FWO-Flanders for a PhD-scholarship.

Author Contributions

Conceptualization: J.V., F.D.V., I.G., F.H., K.K., K.D. and C.V. Data curation: J.V., F.H., J.G., S.D.L., J.B., G.H. and C.V.B. Formal analysis: J.V., F.H., J.G., S.D.L., J.B., G.H. and C.V.B. Investigation: J.V., F.H., S.D.L., J.B. and B.D. Methodology: J.V., F.H., F.D.V., I.G., G.H., C.V.B., K.K. and K.D. Project administration: F.D.V. and I.G. Resources: F.D.V., I.G., J.V.D.E. and S.V.C. Software: J.V., J.B., C.V., F.H. and J.B. Supervision: K.D., C.V., J.V.D.E., S.V.C., I.G. and F.D.V. Validation: J.V., S.D.L., F.H., K.K. and C.V.D.B. Visualization: J.V., J.B., F.H., C.V. and B.D. Writing - original draft: J.V. and F.H. Writing - review & editing: J.V., F.H., K.K., J.B., S.D.L., J.G., B.D., G.H., C.V.D.B., K.D., C.V., J.V.D.E., S.V.C., I.G. and F.D.V.

Additional Information

Supplementary information accompanies this paper at <https://doi.org/10.1038/s41598-019-40013-x>.

Competing Interests: The authors declare no competing interests.

Publisher's note: Springer Nature remains neutral with regard to jurisdictional claims in published maps and institutional affiliations.



Open Access This article is licensed under a Creative Commons Attribution 4.0 International License, which permits use, sharing, adaptation, distribution and reproduction in any medium or format, as long as you give appropriate credit to the original author(s) and the source, provide a link to the Creative Commons license, and indicate if changes were made. The images or other third party material in this article are included in the article's Creative Commons license, unless indicated otherwise in a credit line to the material. If material is not included in the article's Creative Commons license and your intended use is not permitted by statutory regulation or exceeds the permitted use, you will need to obtain permission directly from the copyright holder. To view a copy of this license, visit <http://creativecommons.org/licenses/by/4.0/>.

© The Author(s) 2019